frontiers in Marine Science

TYPE Original Research
PUBLISHED 21 May 2026
DOI 10.3389/fmars.2026.1817180

Check for updates

OPEN ACCESS

EDITED BY
Saravana Periaswamy Sivagnanam,
Munster Technological University, Ireland

REVIEWED BY
Mostafa Mohamed El-Sheekh,
Tanta University, Egypt
Suresh Veeraperumal,
Upstate Medical University, United States
Ge Zhao,
Southwest Medical University, China
G.S. Anisha,
Government College for Women, India
Saima Mirza,
University of Education Lahore, Pakistan

*CORRESPONDENCE
Santhiyagu Prakash
algaprakash@gmail.com;
prakash@tnfu.ac.in

RECEIVED 25 February 2026
REVISED 23 April 2026
ACCEPTED 23 April 2026
PUBLISHED 21 May 2026

CITATION
Mahapatra S, Ramasubburayan R, Durairaj T, Bharathi S, Ramanathan G, Kannapiran E, Immanuel G, Anand C and Prakash S (2026) Deciphering the multifunctional bioactivities of ulvan from *Ulva lactuca*: structural insights with emphasis on antibiofilm and cytotoxic properties.
Front. Mar. Sci. 13:1817180.
doi: 10.3389/fmars.2026.1817180

COPYRIGHT
© 2026 Mahapatra, Ramasubburayan, Durairaj, Bharathi, Ramanathan, Kannapiran, Immanuel, Anand and Prakash. This is an open-access article distributed under the terms of the Creative Commons Attribution License (CC BY). The use, distribution or reproduction in other forums is permitted, provided the original author(s) and the copyright owner(s) are credited and that the original publication in this journal is cited, in accordance with accepted academic practice. No use, distribution or reproduction is permitted which does not comply with these terms.

Deciphering the multifunctional bioactivities of ulvan from *Ulva lactuca*: structural insights with emphasis on antibiofilm and cytotoxic properties

Sonalismita Mahapatra[1], Ramasamy Ramasubburayan[2], Thirumurugan Durairaj[3], Selvaraj Bharathi[4], Ganesan Ramanathan[5], Ethiraj Kannapiran[6], Grasian Immanuel[7], Chandran Anand[8] and Santhiyagu Prakash[8,9]*

[1]Department of Fisheries Biotechnology, Institute of Fisheries Post Graduate Studies, Tamilnadu Dr. J. Jayalalithaa Fisheries University, Chennai, Tamil Nadu, India, [2]Department of Prosthodontics, Saveetha Dental College and Hospitals, Saveetha Institute of Medical and Technical Sciences (SIMATS), Saveetha University, Chennai, Tamil Nadu, India, [3]Department of Biotechnology, Faculty of Science and Humanities, SRM Institute of Science and Technology, Kattankulathur, Chengalpattu, Chennai, Tamil Nadu, India, [4]Centre for Modern Organic Agriculture Research (CMOAR), Sathyabama Institute of Science and Technology, Chennai, Tamil Nadu, India, [5]Postgraduate and Research Department of Microbiology, Sri Paramakalyani College, Alwarkurichi, Tamil Nadu, India, [6]Department of Zoology, Centre for Distance and Online Education, Alagappa University, Karaikudi, Tamil Nadu, India, [7]Centre for Marine Science and Technology (CMST), Manonmaniam Sundaranar University, Rajakkamangalm, Tamil Nadu, India, [8]Mandapam Centre for Sustainable Aquaculture (MCeSA), Directorate of Sustainable Aquaculture (DSA), Tamilnadu Dr. J. Jayalalithaa Fisheries University, Ramanathapuram, Tamil Nadu, India, [9]Marine Biotechnology Research Laboratory, Department of Basic Sciences, Institute of Fisheries Post Graduate Studies, Tamilnadu Dr. J. Jayalalithaa Fisheries University, Chennai, Tamil, Nadu, India

Background: The increasing prevalence of antimicrobial resistance (AMR), alongside the growing incidence of cancer, diabetes and adverse effects associated with antibiotics, chemotherapy and synthetic drugs, encourages researchers to find out natural products as a potential solution. In this context, a systematic approach was applied to extract ulvan from the edible green algae *Ulva lactuca*, known for its rich biochemical composition and to determine its multifunctional biomedicinal properties.

Methods: In this study, sulphated polysaccharide ulvan was extracted from *U. lactuca* through hot water extraction and the purified ulvan was characterized by various spectral analysis. Biomedical properties of the ulvan were determined through *in vitro* assays approaches. The biocompatibility of the ulvan was assessed by Artemia cytotoxicity and anticancer activity against human skin cancer (A431) cells.

Results: The organoleptic characteristics of ulvan revealed that it is odourless, whitish in colour, polar, powdery, and possesses gelling ability. Biochemical analysis indicated that ulvan exhibited high thermal stability under conditions ranging from 103.6 to 600 °C, with a near-neutral pH of 6.7–7.4, and contained substantial amounts of carbohydrates, alongside sulfate groups, uronic acids, and proteins. Spectroscopic analysis revealed the structural makeup and functional groups of the ulvan. The extracted ulvan exhibited promising free-radical scavenging activity (DPPH, FRAP, HPO, and TAA). Antimicrobial studies revealed that ulvan inhibited both bacterial and Candida strains, with MICs in the range of 50 to 90 µg/mL. It had also exhibited notable antibiofilm activity, as evidenced by

inhibition of exopolysaccharide production, increased protein leakage, and ROS production in the tested pathogens, along with microscopic visualization confirming eradication of microbial adherence on glass surface. *In vitro* antidiabetic activity of ulvan showed promising α-amylase inhibitory activity, with an IC_{50} of 78.43 µg/mL. The safety assessment of ulvan revealed minimal toxicity to *Artemia salina* nauplii (LC_{50}: 147.8 µg/mL). The cytotoxicity of ulvan on A431 cells recorded an IC_{50} value of 82.44 µg/mL.

Conclusion: Overall, this study elucidated the structural and biomedicinal attributes of ulvan, notably revealing its pronounced antibiofilm activity and selective cytotoxic effects against human skin cancer (A431) cells remains comparatively underexplored. Hence, this study substantiates its potential as a promising multifunctional therapeutic applications.

KEYWORDS

marine algae, *Ulva lactuca*, ulvan, sulphated polysaccharide, biomedical applications, good health and well being

1 Introduction

The abundance of marine environments on Earth provides opportunities for sustainable use across various sectors. The pelagic zone primarily consists of primary producers, such as seaweed (Red, Brown, and Green). These seaweeds offer a unique nutritional profile, containing proteins, polysaccharides, phenolic compounds, iodine, bromine, and antibiotics, making them a superfood. The rising global demand for seaweed presents opportunities for its cultivation and export. China, Japan, and the USA are the leading importers, while the primary producers and exporters are China, Indonesia, and the Republic of Korea (Akter et al., 2024). Green seaweeds are recognized as edible and non-toxic compared to red and brown seaweeds, yet they have not been thoroughly explored. *Ulva* spp., *Enteromorpha* spp., *Chaetomorpha* spp., *Codium* spp., and *Caulerpa* spp. are some of the typical green seaweeds. *Ulva* spp., is one of the predominant green seaweeds that thrives in different parts of the world such as Europe, North America and South America, the Caribbean, Africa, the Indian Ocean, South-West Asia, China, the Pacific, Australia, and New Zealand, among others, providing an avenue to study the various species of seaweeds with the view to using them sustainably and improving human lives (Tian et al., 2015). India harbors a vast seaweed resource from the eastern seashore to the southern coastal areas. The Veraval and Gulf of Mannar coastal regions of India host rich seaweed biodiversity, including the major groups *Ulva* spp., *Chaetomorpha* spp., *Bryopsis* spp., and *Gracilaria* spp.

In recent years, marine polysaccharides derived from marine resources such as seaweeds, crustaceans, fish and marine invertebrates have attracted immense interest due to their wide range of biological activities (Pramanik et al., 2024; Jeyachandran and Aman, 2025; Ravi et al., 2025). In particular, the sulfated polysaccharide ulvan obtained from genera of green has been reported to exhibit numerous biomedical properties (Wang et al., 2023; Xu et al., 2023; Kraiem et al., 2024). Recently, Shimabukuro et al. (2025) demonstrated a promising immunomodulatory effect of ulvan oligosaccharides derived from green algae and attributed it to the expression of multiple interleukins (ILs) and colony-stimulating factors (CSFs). Likewise, sulphated polysaccharides derived from the green alga *Enteromorpha prolifera* have been reported to induce nitric oxide release in RAW 264.7 cells, stimulate the expression of multiple cytokines, and play a pivotal role in modulating various immune responses (Kim et al., 2011). Similarly, the polysaccharide isolated from *Caulerpa lentillifera* was found to elevate the activity of RAW 264.7 macrophages and further increase nitric oxide production in mice (Sun et al., 2018). In addition to immunomodulatory activity, sulfated polysaccharides, such as sulfated rhamnans from *Monostroma angicava* have been shown to exhibit promising anticoagulant activity (Zhang et al., 2022).

Kraiem et al. (2024) unveiled that sulfated polysaccharides obtained from green algae *Halimeda tuna* exerted noteworthy free-radical scavenging, anti-inflammatory and immunomodulatory activities by altering oxidative stress, stabilizing cell membrane, inhibiting pro-inflammatory mediators and interacting with key targets *viz.* COX-2 and TNF - α. Studies have also shown that sulfated polysaccharides are a promising source of anticoagulants. For instance, the polysaccharide ulvan obtained from *Ulva rigida* through hot water extraction have shown enhanced anticoagulant activity upon sulfation, which significantly impeded intrinsic and extrinsic coagulation pathways and exhibited antithrombin-mediated inhibition of factor Xa and thrombin with efficacy surpassing the standard anticoagulant Lovenox (Adrien et al., 2019). Qin et al. (2023) evidenced that the sulphated polysaccharide from *Chaetomorpha aerea* possesses strong anticoagulant activity by elevating APTT and TT, inhibiting coagulation factors and suppressing thrombin and factor Xa via heparin cofactor II and antithrombin III pathways. Rizk et al. (2016) investigated the effect of sulfated polysaccharide ulvan derived from *Ulva fasciata* on hypercholesterolemia induced in rats and showed that ulvan significantly reduced total cholesterol and LDL, while elevating high-density lipoprotein (HDL). Besides lipid regulation, the ulvan has shown organ-protective effects, as evidenced by a marked reduction in serum urea and creatinine levels, thereby highlighting its renoprotective properties. Ren et al. (2022) formulated a multifunctional ulvan-based hydrogel (derived from *Ulva fenestrata*) and demonstrated its potent antioxidant, antibacterial, and cell-

proliferative properties, markedly accelerating diabetic wound healing *in vivo*. The wide spectrum of bioactivities reported in sulfated green polysaccharides makes them attractive targets for pharmaceutical and nutraceutical development.

Human health and the environment are two primary global concerns that prompt industries to produce eco-friendly products. Although synthetic polymers have been utilized for centuries to meet global demand in the medical and food sectors, in recent times, green synthesis is gaining more attention to reduce pollution. In particular, the use of natural polysaccharides is increasingly recognized for their non-toxic, easily degradable, hydro-gelling, and biocompatible properties compared to chemically synthesized polymer alternatives. In this context, polysaccharides derived from seaweed are gaining immense attention due to their promising biological activities and minimal side effects. Among these, sulfated polysaccharides are notable for their remarkable biological activities, particularly antimicrobial and antiviral properties. For instance, sulfated polysaccharides, *viz*., fucoidan, ulvan, and carrageenan, play a critical role in stimulating an immune response in host cells by activating natural killer (NK) cells. Akter et al. (2024) emphasized that sulfated polysaccharides exert substantial activity against the COVID-19 virus. Moreover, viruses such as the human immunodeficiency virus (HIV), hepatitis C virus (HCV), dengue virus (DENV), herpes viruses (HSV-1 and HSV-2), human papillomavirus (HPV), and various respiratory tract viruses were also reported to be effectively managed using sulfated polysaccharides (Farsimadan and Motamedifar, 2021). Another concern regarding human health is the rising antimicrobial resistance (AMR) genes caused by the overuse of antibiotics. The severity of antimicrobial resistance is underscored by the 4.95 million fatalities attributed to bacterial AMR in 2019, emphasizing the urgent need for effective interventions (Kang et al., 2022). Biofilm formation is a primary factor in the development of bacterial diseases and AMR. Biofilms, which are organized communities of bacteria enveloped in a self-produced exopolysaccharide matrix, create a protective environment that enhances bacterial survival against antimicrobial drugs and the host immune system. In recent days, infections related to biofilms have been identified as chronic, leading to recurrent infections, requiring long-term hospitalization to eliminate these infections, and in severe cases, may require surgical intervention alongside medical therapy (Bjarnsholt et al., 2018).

In general, the nutritional quality of seaweed varies with environmental conditions, season, and species (Xu et al., 2023). Ulvan, a sulfated polysaccharide derived from green seaweed, particularly from *Ulva* spp., has been reported to have diverse applications in the fields of cosmeceuticals, pharmaceuticals, medical, agriculture, textile, food, and aquaculture. Ulvan mainly consist of sulfate and sugars such as rhamnose, xylose, and glucuronic acid. Furthermore, mannose, galactose, glucose, and arabinose are also present to a limited extent. One of the key advantages of ulvan is its structure and charge density, which allows it to dissolve in water, making it a more effective polysaccharide (Pari et al., 2025). Thus, ulvan has unique structural features and heterogeneous sugar compositions that distinguish it from the polysaccharides (agar, carrageenan, and alginate), derived from red and brown seaweeds. The biomedical applications of ulvan include antiviral, antibacterial, free-radical scavenging, anti-inflammatory, immunomodulatory, anticoagulant, hypolipidemic, gastrointestinal, regenerative, and antihyperplasia properties (Pari et al., 2025). Although ulvan derived from various *Ulva* spp. has been investigated, its biological activities are highly influenced by environmental factors and geographical origin, which significantly affect its physico-chemical characteristics, composition and functionality. In this context, in addition to investigating ulvan extraction, organoleptic and structural characteristics, conventional antimicrobial and free-radical scavenging properties, we assessed its antibiofilm activity against clinically important pathogens, membrane damage via protein leakage, EPS inhibition and cytotoxicity against human skin cancer (A431) cells. These additional *in vitro* bioactivity assessments provide a comprehensive understanding of its functionality, which remains comparatively underexplored.

2 Materials and methods

2.1 Collection and identification of *Ulva lactuca*

The fresh and healthy green seaweed *U. lactuca* was collected from Thonidurai, Mandapam coastal regions (9°17'20.89" N; 79° 17'20.89" E) during the post-monsoon at 7.00 AM, and identified using standard keys reported by Umamaheswara Rao (1987). The salinity of the source water during collection was in the range of 30–32 PSU, and the temperature was around 27-29 °C. The collected *U. lactuca* was washed with seawater to remove dirt or any sand particles. It was brought to the laboratory and washed with running tap water, then with distilled water, to ensure complete removal of dust particles. The sample was preserved and kept in the herbarium (Voucher specimen No: MBR-SP-SW-UL-015-2024) at the Marine Biotechnology Research Laboratory, Department of Basic Sciences, Tamilnadu Dr. J. Jayalalithaa Fisheries University, Chennai, Tamilnadu, India. Cleaned *U. lactuca* were shade-dried at room temperature for 10 to 15 days, then dried at 45°C for 4 h to remove excess moisture. The dried *U. lactuca* samples were powdered using a mechanical blender and then stored in a tight glass jar for ulvan extraction.

2.2 Extraction and partial purification of ulvan from *U. lactuca*

In the present study, ulvan was extracted from *U. lactuca* using the hot-water extraction method described by Moawad et al. (2022). Briefly, the depigmentation of the dried *U. lactuca* powder was performed with a mixture of 80% ethanol and dichloromethane, followed by extraction with hot distilled water. Thereafter, ulvan was precipitated using ethanol and then dried. The precipitated ulvan was partially purified via hydrolysis using diluted hydrochloric acid (0.05M), followed by neutralization and crystallization to obtain a dried powder. The ulvan yield (%) was calculated by following Figueira et al. (2020). The elaborate methodology was described in the Supplementary File 1.2, 1.2.1.

2.3 Characterization of ulvan

2.3.1 Organoleptic and solubility of ulvan

The partially purified ulvan was subjected to organoleptic evaluation including colour, odour, taste, texture and ability to dissolve in solvents of varying polarity. The colour was mapped using Munsell chart. The other sensory traits such as odour, taste and texture were determined through simple sensory and tactile trials (Jiao et al., 2011; Kidgell et al., 2019; Tanna and Mishra, 2019). The solubility of the ulvan was determined by ultrasonication at 40° C using an AU33-3.10 ultrasonic bath (ANALAB, India) through visual observation (Lahaye and Robic, 2007). The elaborate methodology was provided in Supplementary File 2.3.1.

2.3.2 Biochemical composition

Biochemical composition of partially purified ulvan was determined using standard procedures. Carbohydrate, protein, sulfate, uronic acid, moisture, ash, and pH were determined using standard tests (Lowry et al., 1951; Hedge and Hofreiter, 1962; Filisetti-Cozzi et al., 1991; AOAC, 2005; Barakat et al., 2022; Lahaye and Robic, 2007). The elaborate methodology is provided in Supplementary File 2.3.2.

2.3.3 Hydrolysis of partially purified ulvan

Hydrolysis of the partially purified ulvan was performed by adding 6M trifluoroacetic acid (TFA) at 100°C for 24 h to convert the polysaccharide into monosaccharide components. After hydrolysis, the content was centrifuged at 3000 rpm for 30 min, and the precipitate was discarded, and the supernatant was utilized for the analysis (Wang and Copeland, 2015).

2.3.4 Analysis of monosaccharide constituents by thin layer chromatography

TLC was applied to find out the composition of monosaccharides in the hydrolyzed ulvan. Briefly, the TLC was carried out using silica 60 F_{254} aluminum-coated sheet as the stationary phase and the following solvent system n-butyl alcohol, acetic acid, and distilled water (6:3:1) as the mobile phase (Jiang et al., 2019). To determine the monosaccharide composition, reference standards such as fructose, maltose, arabinose, fucose, L-rhamnose, D-mannose, D-galactose, and glucose were used. Finally, the developed TLC plates were visualized by spraying sulfuric acid and methanol (1:1) under a UV chamber (590 nm) (CAMAG UV Cabinet 4).

2.4 Structural characterization of partially purified ulvan from *U. lactuca*

2.4.1 UV-Vis spectrophotometry and fourier transform infrared spectroscopic analysis

The partially purified ulvan was subjected to UV-Vis spectrophotometry to determine its maximum absorbance (λ-max) in the range of 200 nm to 800 nm. The FT-IR spectra were recorded in the range of 4000-400 cm^{-1} to identify the functional groups (Kemp, 1991). The procedure is elaborated in Supplementary File 1.4.1.

2.4.2 Nuclear magnetic resonance analysis

The structural properties of partially purified ulvan were determined using ^{1}H and ^{13}C NMR on a Bruker Avance III type 500MHz spectrometer at National Institute of Technology (NIT), Tiruchirappalli. The dissolution of the partially purified ulvan was performed in deuterium oxide (D_2O) to have a definite level of solution. Standard pulse sequences were performed under controlled conditions to collect spectral data and facilitate post-acquisition processing using Mestranova software. Acetone was used as a reference for chemical shifts and fingerprints, and ^{1}H and ^{13}C NMR resonances were observed, disclosing critical structural elements of ulvan (Ciancia et al., 2007). Methods are detailed in Supplementary File 1.4.2.

2.4.3 X-ray diffraction analysis

The dried ulvan sample was ground into a fine powder (<100μm) and uniformly compacted into the sample holder. XRD scans were performed using Cu Kα radiation (1.5406 Å) over a 5°–60° (2θ) range with 0.02°–0.05° steps at 1–2°/min. Diffraction patterns were analyzed to match crystalline phases, with d-spacing determined via Bragg's Law and crystallinity assessed by peak width (FWHM). Quantitative phase analysis, such as the Rietveld method, was employed further to evaluate the proportions of crystalline and amorphous phases and crystalline index (CI). Methods are detailed in the Supplementary File 1.4.3.

2.4.4 Thermogravimetric analysis

The thermal properties of ulvan were determined using a Thermogravimetric analyzer (TGA). The ulvan powder was first dried at 105 °C to remove moisture and determine the accurate weight loss. In brief, the TGA was performed from 25 °C to 1000 °C at a slow heating rate @ 10 °C per minute. During each stage of the temperature rise, the weight loss was recorded as a function of temperature to determine various stages of thermal degradation: moisture evaporation, organic decomposition and residue formation. The TGA graphs were finally used to ascertain the decomposition and thermal stability of ulvan. Methods are detailed in Supplementary File 1.4.4.

2.5 *In vitro* biomedicinal properties of partially purified ulvan

2.5.1 Antioxidant activity

In vitro antioxidant activities of ulvan were determined using DPPH, FRAP, H_2O_2 scavenging and total antioxidant activity as described by Rajivgandhi et al. (2021) and Prakash et al. (2016, Prakash et al., 2023). Gallic acid was used as the positive control. The detailed method is provided in Supplementary File 1.5.1.

2.5.2 Antimicrobial activity

2.5.2.1 Selection of pathogenic microbes

A broad range of clinically relevant microbial strains was selected for the present study to determine the antimicrobial activity of ulvan. Gram-positive bacterial pathogens such as *Bacillus subtilis* (ATCC 6051), *Pseudomonas fluorescens* (ATCC 13525), and Gram-negative strains such as *Staphylococcus aureus* (ATCC 25923). *Enterobacter cloacae* (MG913261) and *Proteus mirabilis* (MG90562). The fungal pathogens used include *Candida albicans* (MTCC 3017) and *Candida tropicalis* (MTCC 184). The detailed description is provided in the Supplementary File 1.5.2.1.

2.5.2.2 Antimicrobial activity, minimal inhibitory concentrations and minimal bactericidal/candicidal concentrations

The antimicrobial activity of ulvan was determined by Lucien et al. (2023) using a 96-well microplate. Briefly, the test microbial suspensions were re-adjusted to 0.5 McFarland (1×10^8 CFU/mL for bacterial cells and 1×10^6 CFU/mL for Candida) (McFarland, 1907; CLSI (Clinical and Laboratory Standards Institute), 2015), and different concentrations of ulvan (25-150 µg/mL) were added to the wells. Streptomycin (20µg/mL) and Fluconazole (20µg/mL) were used as positive controls. After incubation, the growth inhibition was observed, and their MIC was estimated on the basis of a resazurin-based color change. The agar plates were sub-cultured to confirm the MBC/MCC values (Prakash et al., 2015; Ramasubburayan et al., 2023). The elaborate methodology is provided in Supplementary File 1.5.2.2.

2.5.2.3 Biofilm inhibitory activity

The antimicrobial properties of ulvan were measured using a micro-well dilution test (Durgadevi et al., 2019; Divya et al., 2021). Briefly, the bacterial pathogens were grown in TSB (1×10^8 CFU/mL) and Candida in TSB (1×10^6 CFU/mL) and then exposed to different concentrations of ulvan (25–150 µg/mL). The biofilms formed were then stained and solubilized with 0.4% crystal violet in ethanol. The optical density was then measured at 595 nm, and the percentage of biofilm inhibited was calculated and recorded. The detailed method is outlined in the Supplementary File 1.5.3.

2.5.2.4 Quantification of protein leakage

The effect of ulvan on protein leakage by the test pathogens was studied by following method described by Divya et al. (2021). The test pathogens were grown in TSB containing 2.5% sodium chloride with 125 µg/mL (80% BIC) of ulvan and incubated at 37 °C. The culture supernatant was collected at various time intervals 3 -18 h for bacterial pathogens and 12-60 h for *Candida* strains and the protein leakage was measured at 660 nm with BSA as a standard. The Supplementary File 1.5.4 describes a detailed methodology.

2.5.2.5 Quantification of extracellular polymeric substances

The extracellular polymeric substances (EPS) were determined by a modified method described by Jeesha et al. (2024). The bacterial and candidal strains were individually added to 0.5 ml of TSB, which was supplemented with 2.5% NaCl and subsequently, 125 µg/mL ulvan was added and incubated at 37 °C. Thereafter, cell pellets were collected at varying time intervals, and EPS was precipitated by adding ice-cold ethanol. The sample was then incubated at -20 °C overnight. The content of EPS in carbohydrates was assessed by means of a colorimetric test. The detailed methodology is provided in Supplementary File 1.5.6.

2.5.2.6 Quantification of reactive oxygen species (ros) on pathogenic bacterial strains treated with ulvan

Reactive oxygen species (ROS) production was followed by the method described by Becerra et al. (2003) and Hou et al. (2024). The test microbial strains were individually resuspended in Hank's Balanced Salt Solution (HBSS) and mixed with different concentrations of ulvan (50-150 µg/mL) in the presence of nitro blue tetrazolium (NBT). To quantify the amount of ROS produced, the reaction was quenched with HCl after incubation at 37 °C in the dark for 30 min, after which the absorbance was read at 575 nm. The detailed methodology is outlined in the Supplementary File. 1.5.7.

2.5.2.7 Determination of antibiofilm architecture

The efficacy of ulvan (125 µg/mL) on biofilm formation by test pathogens was determined by Durgadevi et al. (2019) and Prakash et al. (2023). Briefly, the biofilms formed were stained with 0.4% crystal violet reagent and 0.1% acridine orange stain, and the stained glass pieces were viewed under a light microscope and a Confocal Laser Scanning Microscope (CLSM). The elaborate procedure is described in the Supplementary File. 1.5.8.

2.5.3 *In vitro* antidiabetic (α-amylase inhibition) assay

The commercially available porcine pancreatic amylase (A4268-25MG, Sigma-Adrich, India) was used for α-amylase inhibitory activity of ulvan (Unuofin et al., 2018; Ogunyemi et al., 2022). Briefly, ulvan (12.5 -125 µg/mL) and acarbose (2.5 – 60 µg/mL) were pre-incubated at 37 °C with amylase (0.1 mg/mL). The reaction was started by the addition of starch, incubated for 30 min, after which 1M HCl was added to stop the reaction and the absorbance was read at 580 nm to calculate the inhibition (%) of amylase. The detailed procedure is elaborated in the Supplementary File. 1.5.9.

2.5.4 Biocompatibility of ulvan

2.5.4.1 *Artemia* cytotoxicity assay

The cytotoxic of ulvan against *A. salina* nauplii was studied by Prakash et al. (2023). For the present study, Artemia cysts were purchased from MAF Peqon suppliers. Briefly, varying concentrations of ulvan (50-200 µg/mL) were added to 24-well plates, which were then evaporated at room temperature. After rehydration with filtered seawater containing 10 live nauplii per well, the plates were incubated for 24 h at 25 °C, survival was recorded, and mortality

(%) was calculated as LC_{50} using probit analysis. The elaborated methodology is provided in the Supplementary File. 1.6.1.

2.5.5 Cytotoxicity assessment of human skin cancer (A431) cell line

The A431 human skin adenocarcinoma cell line (NCCS, Pune, India) was cultured in high-glucose DMEM supplemented with 10% FBS and 1% antibiotic-antimycotic at 37 °C in a 5% CO2 incubator (PAS 24-31). At a cell confluency of approximately 80%, cells were trypsinized (0.025% trypsin, 0.01% EDTA), and the cell count was enumerated with a haemocytometer before seeding cells in T25 flasks to go ahead with cell-based assays. This experiment was carried out *in vitro* using the commercially available A431 human skin adenocarcinoma cell line, procured from the National Centre of Cell Science (NCCS), Pune, India. Direct human or animal involvement was not required, as no human or animal subjects were included in the study; thus, the institutional and national guidelines did not require ethical approval or informed consent.

The MTT assay was used to quantify the cytotoxic effect of ulvan in the human skin cancer cell line A431 (human skin adenocarcinoma cell line. The A431 cells were exposed to ulvan (12.5, 25, 50, 75, and 100 µg/mL), and the cell viability (observed by the absorbance of solubilized formazan at 570 nm) was determined after 24 h. The AAT BioQuest calculator was used to determine the IC50. The elaborate procedure is given in the Supplementary File. 1.6.2.

2.5.5.1 Dual staining (AO/EtBr)

In brief, A431 skin cancer cells were exposed to 84.44 µg/mL ulvan (IC_{50} value) and doxorubicin (positive control). Cells were stained using an Acridine Orange: Ethidium bromide mixture to identify the live and dead cells after 24 h. Fluorescence microscopy was used to determine the live and dead cells. The detailed methodology is provided in the Supplementary File 1.6.2.1.

2.6 Statistical analysis

The data obtained from this study were expressed as mean ± standard deviation (SD) of three replicates (n = 3). Before analysis, the data were tested for normality using the Shapiro-Wilk test and for homogeneity of variance using the Levene test. Since the data met both assumptions ($p > 0.05$), a one-way ANOVA was performed, followed by the Student-Newman-Keuls (SNK) and Dunnett-t *post hoc* tests at a 5% significance level using SPSS version 16.0 (IBM Corp., Armonk, NY, USA). The toxicity of ulvan was determined by probit analysis using the EPA Probit Analysis Program (version 1.5, Cincinnati, USA).

3 Results and discussion

3.1 Extraction of sulphated polysaccharide ulvan

In this study, the sulphated polysaccharide ulvan was extracted from *U. lactuca* using a hot water-based extraction method, and it showed a yield of 15.5 ± 0.63% (Table 1), which is significantly higher than that reported by Li et al. (2018) and Moawad et al. (2022), who obtained 11-11.8% ulvan from the green seaweeds *Enteromorpha intestinalis* and *U. fasciata*, respectively. The significant differences in yield could be attributed to the variations in the lineage of polysaccharide composition in the seaweed cell walls, as well as structural differences between the algae, which are believed to result from species-specific biosynthetic pathways, environmental adaptations, and evolutionary origins (Moawad et al., 2022). Yield (%) can also differ significantly due to the type of solvents used, extraction method, such as ultrasonic, subcritical or high-pressure techniques. This result highlights the importance of the extraction procedures in determining the polysaccharide content recovered from different seaweed species.

3.2 Organoleptic characteristics

The ulvan polysaccharide, extracted from *U. lactuca* exhibit inherent organoleptic properties that are crucial for its functional uses. These sensory characteristics are important for evaluating the safety, quality, and overall acceptability of ulvan as a potent agent in both the food and pharmaceutical industries. The sulphated polysaccharide ulvan showed a whitish appearance, and it was odourless when tested for odour. The taste of the ulvan was salty and had a powdery texture. The solubility test concluded that ulvan is water-soluble and partially soluble in DMSO, whereas the other solvents,

TABLE 1 Organoleptic and biochemical characteristics of partial purified ulvan from *U. lactuca*.

S. no	Parameters	Quantification
Extraction of ulvan		
1	Yield Percentage	15.5 ± 0.63%
Organoleptic Characteristics		
2	Appearance	Whitish
3	Odor	Odor less
4	Taste	Salt and Sweet
5	Texture	Powder
6	Solubility	Distilled water soluble
7	Non-solubility	Ethanol, Hexane, DMSO
Biochemical Characteristics		
8	pH range	6.7-7.4
9	Temperature	103.6 °C to 600 °C
10	Ash Content	1.66 ± 0.15%
11	Moisture Content	0.43 ± 0.07%
12	Protein	11.84 ± 3.52%
13	Carbohydrates	47.04 ± 0.42%
14	Sulfate Content	20.1 ± 2.82%
15	uronic acid content	19.03 ± 1.45%
Qualitative analysis of monosaccharides though TLC		
16	Monosaccharides	Rhamnose, Galactose, and Glucose,

TLC, Thin Layer Chromatography.

like ethanol and hexane, were not able to solubilize the ulvan (Table 1). The sulphated polysaccharide ulvan is fibrous and fluffy in its dry state; upon hydration, it formed a viscous, gel-like material. The gelling ability of ulvan is one of its most remarkable properties, making it a natural thickener or stabilizer. Its rheological properties, specifically pseudoplastic flow under shear, resemble those of well-known hydrocolloids, making it a promising agent for use in food and pharmaceutical formulations (Robic et al., 2009). Lahaye and Robic (2007) reported that ulvan is mildly salty and sweet. It is neither bitter nor sweet, and therefore it fits with other product matrices without changing their flavor profile. All these sensory attributes, such as subtle color, faint marine smell, smooth gel texture, and neutral flavor, reflect ulvan versatility. However, specific industrial applications may require special refining steps to achieve product-specific sensory and functional requirements.

3.3 Biochemical composition of ulvan

In the present study, both carbohydrate and non-carbohydrate components in ulvan were determined by the standard method. Herein, ulvan showed the highest carbohydrate content of 47.04 ± 0.42%, followed by various non-carbohydrate components (Table 1). Among the non-carbohydrate constituents, the sulfate content was significantly higher (20.1 ± 2.82%) than the other components. The sulphate content observed in the present study is higher than that reported by Yaich et al. (2014) and Guidara et al. (2024), who recorded 12.80% and 17% by acid extraction and 14% and 15.88% by enzymatic extraction from the green seaweed *U. lactuca*. The sulfate contents of *U. fasciata* (Moawad et al., 2022), *U. intestinalis* (Kazemi et al., 2023), and *U. lactuca* (Guidara et al., 2021) were also reported to be lower, ranging between 14.92% and 17.22%. Even within the same species, different sulfate concentrations have been reported, which may depend on geographical location, extraction procedure, or laboratory conditions. The relatively high sulfate content observed in the present study highlights the effectiveness of the extraction method. Since sulfate is highly hydrophilic, hot water extraction is more effective than other methods. This substantiates that the degree of sulfate substitution in the polysaccharide chains of the extracted ulvan is relatively high. The presence of sulfate and carboxyl groups in ulvan significantly influences the composition and interaction of other inorganic constituents within the polymer matrix. In addition to coastal and seasonal variations, factors such as temperature and pH also significantly affect the degree of sulfation in polysaccharide chains (Yaich et al., 2014).

The protein content of marine polysaccharides is often due to cell wall contamination, which is particularly noticeable in sulfated polysaccharides. Herein, the results showed that ulvan had significantly higher protein content (11.84 ± 3.52%) (Table 1) compared to the findings of earlier studies. For instance, Guidara et al. (2024) reported protein contents of 1.75%, 1.54%, and 1.24% through acid and enzymatic treatment procedures. The notable variation in protein yield could be attributed to differences in extraction conditions, such as temperature, source solvent, and duration, which affect the degradation and solubilization of polysaccharide-protein complexes.

The lower ash content (1.66 ± 0.15%) (Table 1) observed in this study implies a higher degree of purification and less contamination with non-ulvan polymers when compared to previously reported values for ash content from *U. lactuca* (11.73% to 17.07%) (Costa et al., 2012; Yaich et al., 2014). In general, the purification step plays a pivotal role in reducing ash content, as it aids the removal of inorganic impurities from the sulphated polysaccharide ulvan. In this study, membrane filtration was employed prior to alcohol precipitation, which effectively reduced the ash content, suggesting improved extraction efficiency. These biochemical compositions underscore the effectiveness of ulvan extraction from *U. lactuca*. In particular, the presence of higher sulfate content compared to other biomolecules suggests the potent bioactivity of the extracted ulvan.

3.4 Monosaccharide composition of ulvan

The extracted ulvan showed a higher proportion of carbohydrate than non-carbohydrate content, which is the most typical characteristic feature of the polysaccharides. Monosaccharides, the building blocks of complex carbohydrates, play a vital role in determining the structural and functional attributes of polysaccharides and are therefore central to their compositional analysis. It has been reported that uronic acid is the most abundant and primitive carbohydrate component in ulvan. In this study, the uronic acid content in ulvan was found to be 19.03 ± 1.45% (Table 1). Furthermore, qualitative analysis of monosaccharide composition in the ulvan through the TLC analysis with eight different standards (monosaccharides) revealed the presence of varying monosaccharides. Based on the Rf values, rhamnose, galactose, glucose, fructose, arabinose, and fucose were identified. The Rf value of rhamnose in the extracted ulvan was exactly 0.66, highlighting the prominence of sulfated rhamnose (Figure 1A; Table 2). Rhamnose is also considered the primary sugar constituent in various *Ulva* spp., including *U. fasciata, U. intestinalis, U. compressa*, and *U. prolifera* (Barakat et al., 2022; Moawad et al., 2022; Kazemi et al., 2023). Tian et al. (2015) inferred that the main monosaccharide components of polysaccharides extracted from *U. lactuca* include xylose, rhamnose, and glucuronic acid. In another study, rhamnose and xylose were the major constituents of the polysaccharides extracted by *E. intestinalis* (Li et al., 2018). Similarly, the monosaccharide composition of sulfated polysaccharides derived from the edible red algae *Bangiafusco purpurea* showed galactose as the major fraction, while the minor fraction displayed the presence of uronic acid, arabinose, fucose, xylose, and glucose (Jiang et al., 2019). Although monosaccharide composition was determined by TLC, further studies using high-resolution analytical techniques are essential to accurately determine it and better explore the structure-activity relationship of ulvan.

3.5 Spectral characterization of ulvan extracted from *U. lactuca*

3.5.1 UV-Vis spectroscopic analysis

The initial confirmation of partially purified ulvan was determined through UV-Vis analysis, which recorded maximum

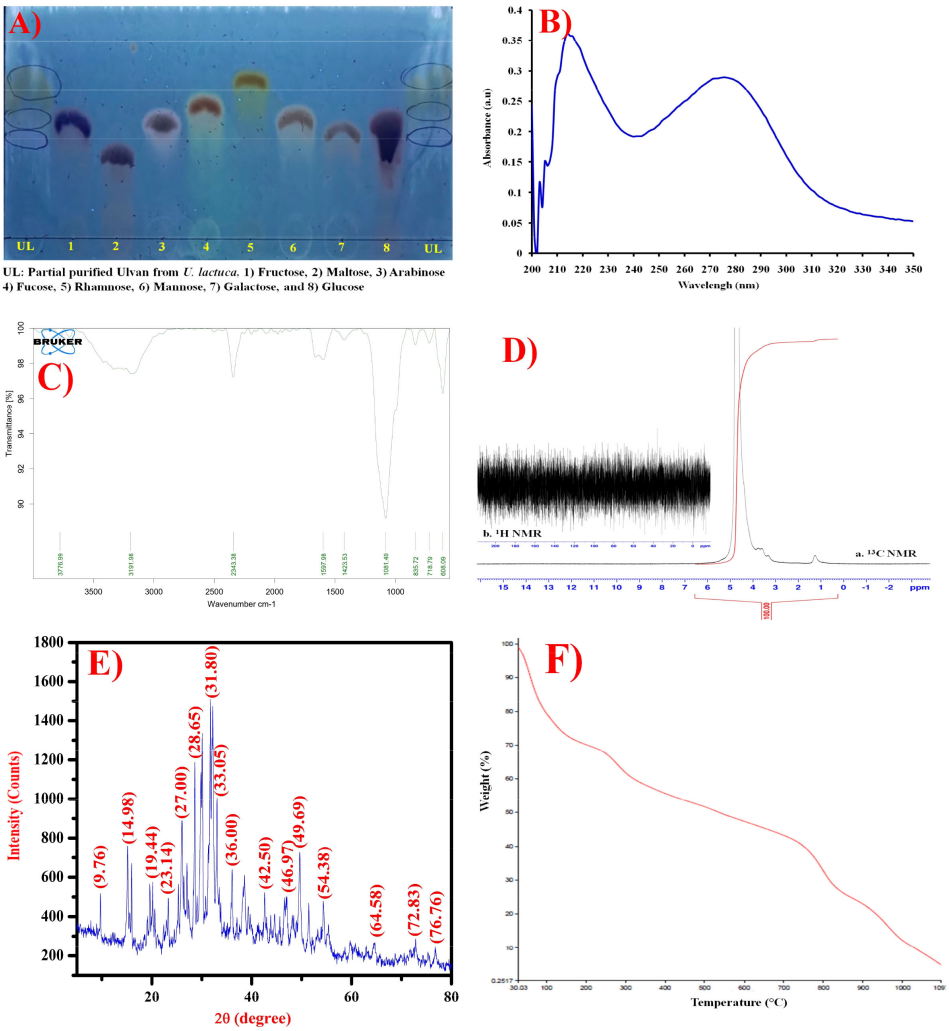


FIGURE 1
Spectroscopic characterization of **(A)** TLC, **(B)** UV- λ max, **(C)** FT-IR, **(D)** C^{13} and ^{1}H NMR, **(E)** XRD, **(F)** TGA analysis of PP- ulvan from *U. lactuca*.

absorbance (λ max) at 215 nm and 280 nm. This indicates the presence of conjugated aromatic systems and ester or carbonyl functionalities within the ulvan molecular structure (Figure 1B). The wavelength regions where the absorption occurs correspond to $\pi \rightarrow \pi$ transition patterns, demonstrating the presence of unsaturated bonds or conjugated structures within the molecule. In line with the results of the present study, UV-Vis results from other studies on ulvan have reported absorbance between 200 and 220 nm (Barakat et al., 2022), indicating the effective extraction of ulvan from *U. lactuca*. Recently, Khaerunnisa et al. (2024) recorded the maximum UV-Vis wavelength of 205 nm for *U. lactuca* derived ulvan. Although the observed absorption is smaller than that of the present study, it falls within the range of 200 – 220 nm.

3.5.2 Fourier transform infrared spectroscopic analysis

Figure 1C illustrates the FT-IR spectra of ulvan. A prominent peak at 3776 cm^{-1} and a broad peak at 3445 cm^{-1} correspond to the

TABLE 2 Quantification of monosaccharides by thin layer chromatography in partially purified ulvan in comparison with reference carbon sources.

S. no	Ulvan/standard carbon sources	Rf values
1.	Partially purified Ulvan from *U. reticulata*	0.46 (Galactose), 0.59 (Glucose), 0.66 (Rhamnose)
Standard Monosaccharides		
2	Fructose	0.48
3	Maltose	0.36
4	Arabinose	0.48
5	Fucose	0.50
6	Rhamnose	0.66
7	Mannose	0.58
8	Galactose	0.46
9	Glucose	0.59

O-H stretch of the hydroxyl group, possibly from rhamnose, xylose and glucuronic acid remnants, which aligns with the previous report by Tian et al. (2015) on the functional groups of ulvan. The peak at 2343 cm^{-1} indicates the C=O stretching of carbon dioxide. The sharp-to-medium-intensity peak at 1597 cm^{-1} indicates the asymmetric stretching of the COO- group in the carboxylate groups of uronic acids, an important acidic component of ulvan. Symmetric stretching of the COO- groups is confirmed by the sharp peak at 1423 $cm^{-1,}$ which further highlights the characteristics of the polysaccharide. Also, the sharp peak at 1081 cm^{-1} corresponds to the stretching of COC bonds representing the glycosidic bonds in the backbone of ulvan. Three medium-intensity peaks at 835 cm^{-1}, 718 cm^{-1}, and 608 cm^{-1} serve as strong indicators of sulfation, particularly in rhamnose or xylose residues, confirming that ulvan is sulfated. These results strongly agree with the functional groups of ulvan determined in other seaweed species described by Rahimi et al. (2016); Barakat et al. (2022); Moawad et al. (2022), and Kazemi et al. (2023). The presence of these functional groups alongside the sulfate group demonstrates the biofunctionality of the extracted ulvan in this study.

3.5.3 Nuclear magnetic resonance analysis

The structural characterization of the partially purified sulphated polysaccharide ulvan was determined through NMR spectroscopy. The results of NMR analysis confirmed its complex sulfate polysaccharide nature, which is illustrated in Figure 1D, Table 3. In the present, the ^{1}H NMR spectra of ulvan showed signals in the range between δ 3.2 and 5.5 ppm, which represents the presence of sugar ring protons and glycosidic linkages. Further, the signals recorded at δ ~ 1.2 and 1.7 ppm are attributed to the methyl protons of rhamnose residues and sulfate esters, which are characteristic of ulvan. Likewise, the ^{13}C NMR spectra of ulvan show prominent peaks at δ 95 to 105 ppm, corresponding to anomeric carbons; 60 – 80 ppm represents the carbonyl carbons from uronic acids, and δ 170 – 180 ppm indicates the presence of carboxyl groups of uronic acids such as glucuronic and iduronic acids. The combined spectral spectroscopic features are in concordance with the presence of ulvan-specific disaccharide repeating units, in particular ulvanobiuronic acid Type A (→ β-D-Glucuronic acids + L-Rhamnose-3-sulfate) and ulvanobiuronic acid Type B (→ α -L- Iduronic acids + L-Rhamnose -3-sulfate), which serve as the backbone of the ulvan. Supporting the results of the present study, Lahaye and Robic (2007) inferred that the Type A and Type B ulvanobiuronic acids were the principal repeating disaccharide units of ulvan, with variations in the composition of glucuronic and iduronic acids driving its structural heterogeneity and functional properties. Similarly, Wahlstrom et al. (2020) reported that marked variation in chemical shifts and signal intensities among Ulva species, extraction methods and environmental conditions reflects the heterogeneous structure of ulvan. Previous literature on the investigation of ulvan from *U. lactuca* and other Ulva species has effectively utilized NMR analysis to show the critical insights into the sulfation pattern, composition of monosaccharide, and glycosidic linkages, and thereby validating its structural integrity (Kidgell et al., 2019; Alves et al., 2013). Thus, the NMR analysis observed in the present study strongly agrees with earlier reports, and affirms the presence of rhamnose rich, sulphated polysaccharide backbone characteristic of ulvan.

TABLE 3 Characterization of ^{1}H and ^{13}C NMR spectral analysis of partially purified ulvan from *U. lactuca*.

NMR spectrum	Chemical shift (ppm)	Assignment
^{1}H NMR	5.0	Anomeric protons in glycosidic linkages
	3.2 - 3.98	Sugar backbone protons (hydroxyl, methine, methylene)
	1.79	Methyl groups, possibly part of rhamnose or sulfate esters
^{13}C NMR	90 - 110	Anomeric carbons in glycosidic bonds
	170 - 180	Carbonyl carbons from uronic acids
	60 - 80	Oxygenated carbons in the sugar backbone

H – NMR, Proton Nuclear Magnetic Resonance spectroscopy; C-NMR, Carbon NMR spectroscopy.

3.5.4 X-ray diffraction analysis

XRD analysis of ulvan revealed a semi-crystalline nature with specific peaks at 2θ values of 9.76°, 14.98°, 19.44°, 23.14°, 27.00°, 28.65°, 31.80°, 33.05°, 36.00°, 42.50°, 46.97°, 49.69°, 54.38°, 64.58°, 72.83°, and 76.76° (Figure 1E). These peaks indicate clear diffraction from X-ray analysis, showing that the polysaccharide has a high degree of molecular order. The XRD analysis and Scherrer equation enable the calculation of the single-crystal size of ulvan by measuring FWHM at peak positions of 27.00° and 49.69°, consistent with previous studies on *U. pertusa* (Gao et al., 2020). The size of ulvan is estimated to be between 10 and 50 nm, matching the typical dimensions of marine-derived polysaccharides. A semi-crystalline form of a sulphated polysaccharide from the brown seaweed *Sargassum polycystum*, with a peak crystalline reflection at 32.60°, was determined by Digala et al. (2022), aligning with the present study. A similar type of result was found for the polysaccharide from the green algae *Codium tomentosum*, with peak crystallinity observed at three different positions (30.7°, 31.7°, and 44.6°), indicating the semi-crystalline nature of the polysaccharide (Türker et al., 2022).

The X-ray diffraction (XRD) analysis showed that mainly crystalline phases were dcalculate (Wt %) in partially purified ulvan, using Quartz (SiO_2) as the most prevalent at 47.3%, Feldspar ($KAlSi_3O_8$) (32.7%), and Kaolinite ($Al_2Si_2O_5(OH)_4$) (14.0%). The other 6.0% was described as an amorphous (non crystalline). The sizes of crystallites were determined by the Scherrer equation but resulted in 29 nm, 32 nm, and 19 nm in favour of Quartz, Feldspar and Kaolinite respectively. It was determined that the Crystallinity Index (CI) is 94.0% and so, the partially purified Ulvan is mostly crystalline, but a small part (6.0%)

is amorphous nature (Supplementary Table S1). These results indicate a large crystalline sample having distinct phases and low amorphous. The ulvan is partially purified and structurally analyzed to reveal a complex composition where highly ordered mineral phases are incorporated in the polysaccharide networks which are themselves the sulfated heteropolysaccharide (Kostas et al., 2021). The observation is in contrast to studies on pure polysaccharide architecture such as carrageenan, which are frequently examined because of their ice recrystallization inhibition traits (Hale et al., 2024). Its composition as Quartz, Feldspar, and Kaolinite indicates that not only the polysaccharide itself but also the accompanying inorganic components probably affect the physical properties of the ulvan. This shifts the emphasis away from studies using polysaccharides alone and prompts a reconsideration of how these mineral phases could influence the bioactivity and functional properties of ulvan, given its structural rigidity and possible effects on molecular interactions (Wang et al., 2023). The distinct quartz at 26.81 and 20.92 equals and kaolinite are similar to other boron-based biological and soil materials (Rempfert et al., 2024). Moreover, a Crystallinity Index (CI) of 94.0% strongly confirms that these well-structured mineral phases play an important role in the overall structural integrity of the material (Patil et al., 2025). The Quartz (29 nm), Feldspar (32 nm), and Kaolinite (19 nm) exhibited nanocrystalline dimensions, as determined using the Scherrer equation. These mineral inclusions may affect the mechanical and surface characteristics of the material, which may affect the performance of the polysaccharide in the application that may necessitate mechanical reinforcement or a particular interfacial phenomenon (Benito-González et al., 2021). This type of ulvan predominates in crystalline phases over less crystalline or semi-crystalline phases, again underscoring the need for further research to understand the contributions of the ulvan and co-occurring minerals to the material's functional characteristics. Future studies are advised to address the relative effect of each component to enhance prediction of the use of the ulvan and functionality.

3.5.5 Thermogravimetric analysis

The TGA analysis of ulvan was performed to ascertain its thermal properties and to understand the degree of dry phosphate-based ulvan, including the dehydration and secondary decomposition, followed by the oxidation process. The first weight loss was observed between room temperature and 103.6 °C, with a 30.03% weight loss, indicating the evaporation of volatile organic compounds and a notable reduction in moisture content. The second stage ranged between 103.6 °C and 600 °C, with almost 45% weight loss resulting in the disruption of glycosidic bonds and the formation of CO_2, CO, and water vapour as volatile compounds. Thereafter, a 5% weight loss during the third stage between 601 and 800 °C implied the decomposition of the remaining stable substances, such as char and inorganic matter, in the sample. The decomposition at higher degree (800-1000 °C) was minimal, showing that the material contained inorganic components that did not break down within this temperature range (Figure 1F). Conversely, Abu-Resha et al. (2026) reported that the TGA results for ulvan extracted from *U. lactuca* indicate significant thermal stability, with weight loss (23.42%) in initial temperature at 40 °C; which was attributed to the removal of moisture and volatile compounds, suggesting that ulvan retains its structure under moderate increasing temperature at above 770 °C, has recorded in a major decomposition temperature. The most significant weight loss noticed in the present study was around 200-300 °C, aligning with the previous reports on *U. lactuca*, *U. fasciata*, and *U. intestinalis*, which reported weight losses at 221 °C, 245 °C, and 226 °C, respectively (Kazemi et al., 2023; Abu-Resha et al., 2026). It was found that 526.08 °C efficiently destroyed inorganic materials in *U. intestinalis*; whereas in the present study, the temperature ranged between 601-800 °C (Kazemi et al., 2023). Above 700-800 °C, ulvan samples may contain substances such as sulfates, phosphates, and carbonates, which are typical of the polysaccharides (Abu-Resha et al., 2026).

In general, the biological activity of ulvan mainly depends on its molecular weight distribution, which often regulates its physicochemical characteristics and interactions with the biological systems. Previous literature on GPC/SEC analysis revealed that the polysaccharide ulvan extracted from *U. panenfusii* and *U. nematoidea via* hot-water extraction method exhibited a relatively homogeneous molecular weight distribution, suggesting preservation of polymer chain integrity. Nevertheless, the extraction of ulvan under alkaline conditions resulted in heterogeneous molecular weight, attributed to partial depolymerization of the ulvan polysaccharide chains (Gonzales et al., 2025a). Moreover, *U. papenfussi*-derived ulvan has been found to show higher molecular weight than *U. nematoidea*, indicating species-dependent structural variability. In a recent study, Gonzales et al. (2025b) inferred that the ulvan derived from various *Ulva* spp. showed a wide molecular weight ranged between 50 and 2000 KDa, merely depending on the type of extraction method and taxonomic origin. Also, a remarkable variation in extraction methods can modulate the structural features viz., the composition of sulfate content and uronic acids, the underlying factors responsible for the biological activities (Sun et al., 2025). Although molecular weight determination has not been carried out in the present investigation, the use of hot-water extraction implies that the obtained ulvan seems to retain a relatively uniform molecular weight distribution, as reported for ulvan extracted from *U. papenfussii* and other *Ulva* species. However, the absence of a GPC/SEC study limits the ability to assess the underlying structure-activity correlation, an important area for future research.

3.6 *In vitro* biomedicinal properties

3.6.1 Antioxidant activity

The antioxidant activity of ulvan is primarily determined by its sulphated polysaccharide content, sulfate level, and molecular weight (Li et al., 2018). Herein, the results of the DPPH scavenging activity showed a steady increase from 31% to 90% with a rise in ulvan concentration from 10 to 100 µg/mL, yielding an IC_{50} of 29.5 µg/mL, which is considerably higher than that of gallic acid (14.91 µg/mL) (Figures 2A, B). Supporting the results of the present study, Kazemi et al. (2023) showed DPPH activity ranged between 50.07% to 73.24%. They observed 60% antioxidant activity at a 100 µg/mL dose of ulvan,

which is comparatively much lower than the present study, which showed 90% at 100 µg/mL. In the hydrogen peroxide assay (HPO), ulvan achieved up to 63% scavenging activity at 100 µg/mL, with activity increasing from 11% to 63% across the test concentration, and an IC_{50} of 77.15 µg/mL compared with 19.56 µg/mL for gallic acid (Table 4; Figures 2A, B). The FRAP assay showed 98% activity, whereas ulvan at 100 µg/mL exhibited 1.8-fold lower activity as reported by Kazemi et al. (2023). The Total antioxidant activity (TAA) of ulvan was higher at 100 µg/mL with 2.79 ± 0.05 mg/g concentration (Figures 2A, B), matching the potential of gallic acid, thereby emphasizing the bioactive role of sulfate groups in polysaccharides (Barakat et al., 2022; Palanisamy et al., 2017). In agreement with the results of the present study, studies on ulvan from several Ulva species such as *U. australis*, *U. rigida* and *U. ohnoi* confirmed appreciable radical scavenging and ROS inhibitory activity (Li et al., 2023; Barakat et al., 2022; Kim et al., 2025). The key mechanism by which ulvan exerts antioxidant activity is based on the presence of sulfate groups and uronic acids, which regulate electron transfer and radical stabilization. For instance, in DPPH assay, ulvan scavenges the radicals through electron donation from sulphated polysaccharide chains, suggesting that a higher sulfation will result in enhanced scavenging activity (KIdgell et al., 2019; Zhang et al., 2019). On the other hand, it has been reported that in the HPO assay, ulvan neutralizes hydrogen peroxide radicals and inhibits ROS formation, thus preventing the generation of hydroxyl radicals, which is claimed to be mediated by sulfate and uronic acid residues (Qi et al., 2005; Alves et al., 2013). In the FRAP assay, ulvan

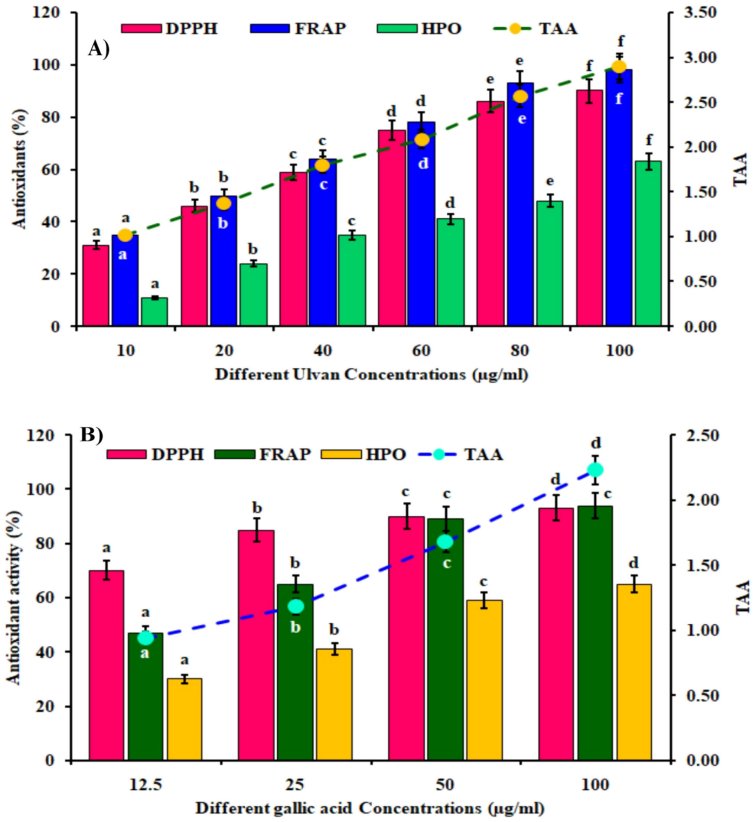


FIGURE 2
Antioxidant activity (DPPH, FRAP, HPO and TAA) of PP-ulvan and gallic acid. Each value is the Mean ± SD of triplicate analysis; each set of bars represents different concentrations of PP-Ulvan **(A)** and Gallic acid **(B)** different concentrations of ulvan and gallic acid with different superscript (a-f) letters are statistically significant (One-Way ANOVA test: $P < 0.05$, further, the *post hoc* multiple comparison with SNK test).

TABLE 4 **Summary of concentrations of BIC_{50}, IC_{50} and LC_{50} values of partially purified ulvan for antibiofilm, antioxidant, α -amylase inhibition, *Artemia* cytotoxicity and MTT cytotoxicity by A431 cells.**

Test compounds	BIC_{50} (µg/mL)							Antioxidant activity (µg/mL)			Amylase inhibition (µg/mL)	Cytotoxicity (µg/mL)	
	BS	EC	PF	PM	SA	CA	CT	DPPH	FRAP	HPO		*Artemia* naupllii	A431 cell line
Partially purified ulvan	72.8	80.5	78.6	67.4	78.5	52.3	78.0	29.5	23.44	77.15	78.43	147.8	82.44
Standard	ND							14.91	6.6	19.56	13.1	ND	ND

Biofilm inhibitory concentrations 50% (BIC_{50}), Inhibitory Concentrations 50% (IC_{50}), Lethal Dose Concentrations 50% (LC_{50}). BS, *B. subtilis*; EC, *E. cloacae*; PF, *P.* fluorescens; PM, *P. mirabilis*; SA, S. aureus; CA, C. albicans; CT, C. tropicalis. ND, Not Done.

was reported to exert reducing power (Fe^{3+} to Fe^{2+}) through electron donation, primarily achieved by the percentage of sulfate content (Costa et al., 2010). The antioxidant results observed in the present study is considerably better than the previous studies, wherein fucoidan fractions isolated from *Hizikia fusiforme*, K-Carrageenan, and K-Carageenan/lignin composite film had an IC_{50} value in the range of 93 µg/mL to 3903 µg/mL (Wang et al., 2020; Rukmanikrishnan et al., 2020). These results indicate that ulvan as a promising free-radical scavenging agent.

3.6.2. Antimicrobial activity

3.6.2.1 Antimicrobial activity and minimal inhibitory concentrations, minimal bactericidal/candicidal concentrations

The results of antimicrobial activity inferred that, at lower concentrations (25, 50, and 75 µg/mL) ulvan showed strong (+++) to minimal (+) growth inhibitory activity against the tested pathogens. However, further increase in concentration (100-150 µg/mL) resulted in complete inhibition (#) of bacterial and candidal growth. The positive control (PC) containing 20 µg/mL of streptomycin and fluconazole completely inhibited the growth (#) of all pathogens. The bacteriostatic (MIC) and bactericidal (MBC) activity of ulvan indicated that the bacterial pathogens *P. fluorescens* (MIC: 50 µg/mL, MBC: 60 µg/mL) and *S. aureus* (MIC: 60 µg/mL, MBC: 70 µg/mL) were the most susceptible strains. In contrast, *E. cloacae, B. subtilis*, and *P. mirabilis*, recorded considerably higher concentrations of ulvan to exert bacteriostatic (70 - 90 µg/mL) and bactericidal (80 - 100 µg/mL) activity. Similarly, the polysaccharide ulvan tested against fungal pathogens *C. albicans* and *C. tropicalis* showed MICs of 80 µg/mL and MBCs of 90 µg/mL, respectively (Table 5). The efficacy of ulvan in inhibiting and eradicating bacterial and fungal pathogens, with antimicrobial activity comparable to the positive control, highlights its potential as an effective alternative antimicrobial agent. Several authors reported that sulfated polysaccharides extracted from seaweed exert pronounced antimicrobial properties against both G^{+ve} and G^{-ve} bacterial pathogens (Sulastri et al., 2021; Kazemi et al., 2023). The extensive range of bacteria that sulfated polysaccharides from seaweed inhibit suggests their potential as effective, nature-based antimicrobial agents. Several investigations have suggested that the antibacterial activity of sulfated polysaccharide ulvan from seaweeds is mediated through multiple mechanisms, wherein i. the sulfated groups of the ulvan adhere to bacterial membranes and disrupt their structural integrity and lead to cell death, ii. it chelates the metal ions essential for the growth, metabolic activity and impedes cellular processes, iii. prevents adherence and colonization of test pathogens and iv. blocks the DNA replication and protein synthesis (Ibrahim et al., 2022; Tziveleka et al., 2022; Anisha et al., 2023; Akter et al., 2024). The antimicrobial activity exerted by the positive control streptomycin and

TABLE 5 Antimicrobial properties, MIC and MBC of partially purified ulvan against selected bacterial and candidal strains.

Ulvan concentration (µg/mL)	B. subtilis	E. cloacae	P. fluorescens	S. aureus	P. mirabilis	C. albicans	C. tropicalis	Chromo variation
Negative Control	+++	+++	+++	+++	+++	+++	+++	
25	+++	++	++	++	+++	++	++	
50	++	+	+	+	++	+	+	
75	+	+	+	+	+	+	+	
100	#	#	#	#	#	#	#	
125	#	#	#	#	#	#	#	
150	#	#	#	#	#	#	#	
PC (20µg/ml)	#	#	#	#	#	#	#	
MIC (µg/ml)	80	70	50	60	90	80	80	
MBC (µg/ml)	90	80	60	70	100	90	90	

+++, Vigorous Growth; ++, Moderate Growth; +, Less Growth; #, No Growth; Chromo variation indicates Yellow to white is excellent growth to no growth, Pink colour indicates Minimal Inhibitory Concentrations (MIC) value, and blue colour indicates Minimal Bactericidal/Candidicidal concentrations (MBC/MCC values). PC, Positive control as Streptomycin for bacterial strains and Fluconazole for *Candida* strains.

fluconazole as indicated by the MIC (50–80 µg/mL and MIC: 80 µg/mL) and MBC (60 - 100 µg/mL and 90 µg/mL), is considerably less than that of the polysaccharide ulvan. This remarkable difference may be attributed to the ulvan's polymeric nature, marginally lower specificity towards test pathogens, and the indirect mechanism of action; additionally, the ulvan used in the present study is a partially purified polysaccharide. Moreover, ulvan exhibits antimicrobial activity primarily through non-specific mechanisms, such as interaction with the cell membrane and inhibition of adhesion, whereas streptomycin specifically targets cellular pathways. Further, when comparing the antimicrobial efficiency of various marine-derived polysaccharides, *viz.* fucoidan, carrageenan, and alginate, the ulvan from *U. lactuca* showed a pronounced antagonistic activity. For instance, fucoidan isolated from *Fucus vesiculosus* L and *Laminaria japonica* exhibited MICs in the range of 4 mg/mL to 8 mg/mL against *E. coli, B. licheniformis, S. aureus* and *S. epidermidis* (Ayrapetyan et al., 2021; Liu et al., 2017).

3.6.2.2 Biofilm inhibitory activity

Biofilm formation is a protective mechanism used by pathogenic microorganisms to withstand adverse conditions, such as antibiotic treatment for bacterial infections. Many bacteria and fungi produce biofilms, increasing their virulence against hosts. Controlling biofilm formation is crucial for eradicating pathogens. In the current study, the results of biofilm inhibitory activity indicated that the polysaccharide ulvan significantly ($P < 0.05$) reduced biofilm in a dose-dependent manner (Figures 3A, B). The biofilm inhibitory activity of ulvan at 25 µg/mL remained low across all bacterial strains, with inhibition rates ranging from 12% to 24%. However, the biofilm inhibitory activity increased notably as the concentration of ulvan rose. For instance, at 50 µg/mL concentration, ulvan inhibited biofilm formation of *P. mirabilis* and *S. aureus* (38%), *B. subtilis* (32%), *P. fluorescens* (30%), *E. cloacae* (23%), and *Candida* strains such as *C. albicans* (41%), and *C. tropicalis* (33%), respectively. This activity increased gradually, and at 150 µg/mL, the biofilm inhibitory test demonstrated 96% effectiveness against *B. subtilis*, while other pathogens, such as *S. aureus*, *P. mirabilis*, and *P. fluorescens*, showed 90% biofilm inhibition. The concentration of ulvan required to inhibit 50% (BIC_{50}) of biofilm formation by different bacterial strains in the present study is as follows: *B. subtilis* (72.8 µg/mL), *E. cloacae* (80.5 µg/mL), *P. fluorescens* (78.6 µg/mL), *P. mirabilis* (67.4 µg/mL), and *S. aureus* (78.5 µg/mL), *C. albicans* (52.3 µg/mL) and *C. tropicalis* (78.0 µg/mL) (Table 4). The biofilm inhibitory property of ulvan confirms that it effectively hinders the formation of biofilms by more than 90% of all test pathogens at 150 µg/mL, thus presenting itself as a suitable alternative for managing antibiotic-resistant bacterial infections and biofilm infections. Corroborating the results of the present study, several authors investigated the biofilm inhibitory properties of sulfated polymers from red and brown seaweed species, e.g, fucoidan and alginate as polysaccharides that efficiently arrest the pathogenic bacterial growth and its associated plaque formation (Negreanu-Pirjol et al., 2022; Behzadnia et al., 2024; Alfinaikh et al., 2025). Earlier reports on the mechanism of biofilm inhibitory activity of sulphated polysaccharides from seaweeds suggest that they i. strongly disrupt quorum sensing (luxS downregulation) between the pathogens, ii. reduce exopolysaccharide synthesis, iii. increase protein leakage, iv. inhibit bacterial adhesion v. downregulate virulence-associated genes (rpoS, hilA, avrA) and thereby resulting in distortion of biofilm architecture and uneven spreading of mature biofilms (Roy et al., 2025; Jun et al., 2018; Rajasekaran and Viswanathan, 2023).

3.6.2.3 Protein leakage

Considering antimicrobial activity, the release of protein leakage by bacterial pathogens due to drug/bioactive molecules suggests pronounced membrane cell disruption. Previous studies have demonstrated that bacterial cell membranes are damaged by polysaccharides, including fucoidan, alginate, and ulvan, leading to the breakdown of intracellular proteins. In this study, we examined the effect of ulvan on protein leakage in the selected test bacterial pathogens at 125 µg/mL concentration over different time intervals (3 - 18 h) (Figures 3C, D). The results of protein leakage inferred that it was 9% for B. subtilis, 26% for E. cloacae, and 20% for P. fluorescens after 3 h. But, after 9 h, protein leakage increased to 69% in B. subtilis, 63% in E. cloacae, and 45% in P. fluorescens. Over time, the protein leakage levels increased across all test strains, with B. subtilis reaching 75%, followed by E. cloacae and P. fluorescens, which reached 78% and 71%, respectively, at the end of 12 h. By 18 h, E. cloacae, P. fluorescens, and B. subtilis recorded maximum protein leakage of 88% to 94%. Other tested pathogens, including S. aureus, P. mirabilis, C. albicans, and C. tropicalis, exhibited a notable increase in protein leakage, ranging from 70% to 96% at different time periods. Coincidentally, Rajasekar et al. (2019) observed a steady increase in protein leakage in Vibrio vulnificus due to Spirulina platensis-derived sulphated polysaccharides. Similarly, the sulfated polysaccharide derived from the green seaweed Caulerpa sertularioides has been shown to increase protein leakage in Vibrio harveyi (Anjali et al., 2022). The sulfated polysaccharide galactan from Eucheuma serra and Gracilaria verrucosa promoted the intracellular protein leakage of protein in E. coli ETEC K88, which was validated by the appearance of 35 kDa and 40 kDa protein bands after exposure to polysaccharides, indicating membrane disruption and intracellular protein leakage. According to Kazemi et al. (2023), sulfated polysaccharides have been reported to bind to bacterial cell surface glycoprotein receptors and modify permeability, thereby impeding the synthesis of proteins and nucleic acids, which in turn leads to the leakage of proteins and DNA from the bacterial cell.

3.6.2.4 Quantification of extracellular polysaccharide

Marine polysaccharides show promising potential in impeding infections associated with biofilm formation. It has been reported that marine-derived polysaccharides such as fucoidan, alginate, and ulvan effectively inhibit exopolysaccharide (EPS production in clinically important biofilm-forming pathogens. In particular, breaking down exopolysaccharides in the biofilm matrix makes bacteria more vulnerable to antimicrobial medications. In the present study, quantification of EPS production in pathogens was investigated by treating it with ulvan (125 µg/mL) across different time intervals (3 to 18 h for bacterial and 12 to 60 h for fungal strains) (Figures 3E, F). Results

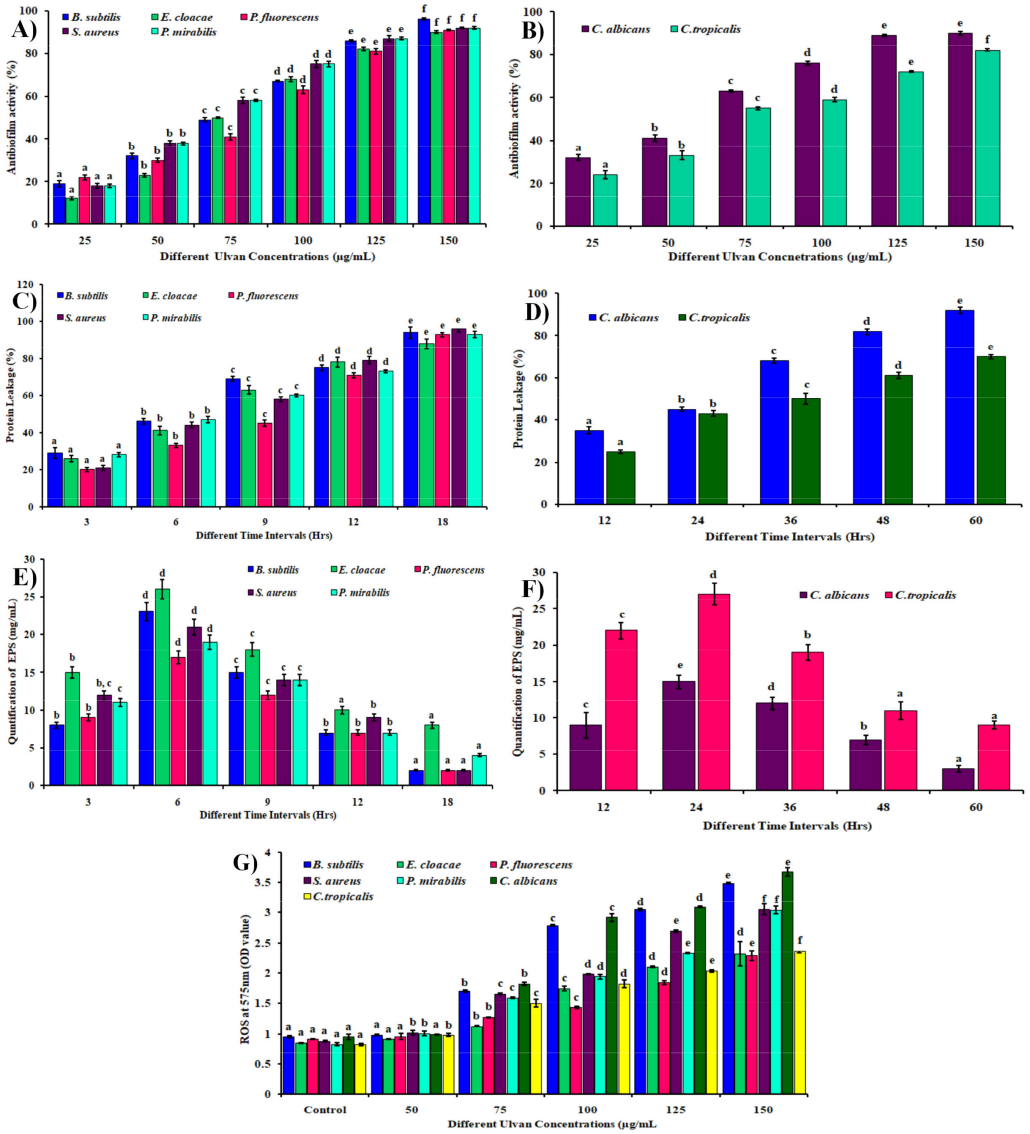


FIGURE 3
Antibiofilm **(A, B)**, Protein Leakage **(C, D)**, EPS **(E, F)**, and ROS **(G)** properties of PP-ulvan against selected pathogens. Each value is the Mean ± SD of triplicate analysis; each set of bars with A&B represents different concentrations of ulvan on antibiofilm activity, **(C, D)** different time intervals on protein leakage and **(E, F)** EPS production, and **(G)** different concentration of PP-Ulvan on ROS activity against selected pathogenic microbes with different superscript letters (a-f) are statistically significant (One-Way ANOVA test: $P < 0.05$, further, the *post hoc* multiple comparison with SNK test).

showed that, after 3 h of incubation, the EPS production was minimal with 8 mg/mL by *B. subtilis*, whereas *C. tropicalis* showed a maximum EPS production of 22 mg/mL at 12 h. However, as the time interval increased from 3 to 6 h, EPS production slightly elevated and was found to be 16-26 mg/mL in *E. cloacae*, 9-19 mg/mL in *C. albicans* (24 h), and 9-17 mg/mL in *P. fluorescens*. The EPS production levels declined significantly after 12 h and 18 h, thus reflecting the efficiency of ulvan. Among the tested pathogens, *B. subtilis* and *C. albicans exhibit*ed lower EPS production compared to the other strains. Overall, the results on EPS quantification implied that pathogens exposed to 125 µg/mL ulvan successfully impaired EPS production and thus highlighting the ulvan's biofilm inhibitory potential. Vishwakarma and Sirisha (2020) reported that sulfated polysaccharides from *Chlamydomonas reinhardtii* reduced EPS production by 5-fold compared to the control in *Salmonella enterica* and *V. harveyi*. Powell et al. (2018) reported that alginates extracted from brown seaweed manage *P. aeruginosa* EPS formation by breaking down its biofilm structure. The antibiofilm effects of fucoidan have received extensive research attention because they inhibit bacterial EPS formation (Behzadnia et al., 2024). The protein leakage results showed that ulvan strongly disrupts the bacterial cell membrane, leading to release of intracellular proteins and other cytoplasmic contents. Furthermore, ulvan disrupts EPS production and structural stability, thus hindering biofilm development. Several authors substantiated that the broad-spectrum antimicrobial property could be attributed to membrane destabilization, release of intracellular contents, EPS repression, and biofilm inhibition (Sulastri et al., 2021; Ibrahim et al., 2022; Pari et al., 2025).

3.6.2.5 Reactive oxygen species

In the present study, ROS production significantly increased ($P < 0.05$) with increasing ulvan concentrations (50-150 µg/mL) across all tested pathogens (Figure 3G). The control group of pathogens (without ulvan) exhibited comparatively lower ROS levels than those with ulvan, ranging from 0.82 to 0.948. However, at 50 µg/mL of ulvan, the ROS levels of the pathogens were found to be in the range of 0.91 to 1.018. At higher concentrations (150 µg/mL), ROS production in the pathogen peaked (1.842 to 3.67), with notably high ROS levels found in *C. albicans* (3.67) and the lowest in *P. fluorescens* (1.842). These findings reveal a positive correlation between ulvan concentration and ROS production, further suggesting that ulvan exhibits antimicrobial properties and effectively generates ROS to destroy pathogens through cellular decay, based on concentration-dependent relationships. The non-toxic quality of ulvan stems from the organism's ability to regulate ROS production in relation to its antioxidant capabilities, enabling ROS to carry out antimicrobial actions without harming host cells. Herein, ulvan demonstrates its non-toxic properties through two distinct mechanisms. It produces ROS selectively, targeting pathogens while maintaining the host's natural oxidative balance. This leads to therapeutic success without causing significant oxidative stress in the host (Jayawardena et al., 2020). The findings of the present study showed that ulvan significantly increased reactive oxygen species production, yet this increase was accompanied by a rise in antioxidant capacity as reflected in the DPPH, FRAP, HPO and TAA assays.

3.6.2.6 Effect of ulvan on biofilm architecture

The effect of ulvan (125 µg/mL) on the biofilm architecture of the test bacterial pathogens was studied using a light and Confocal Laser Scanning Microscope (CLSM). Considering the light microscopic images, the crystal violet staining showed less cell density and a sparse distribution of cells after ulvan treatment compared to control (Figure 4). These results suggest that the polysaccharide ulvan significantly impaired the biofilm-forming ability of the bacterial strains, indirectly indicating that it inhibited EPS production and blocked quorum sensing signals for communication, as evidenced by notable changes in the biofilm architecture. Similarly, AO staining by CLSM revealed a noteworthy reduction in live cells (green colour), implying reduced cell adhesion, and further empty spaces on the glass substrata indicate bacterial cell death. In contrast, the control slide showed rigid biofilm formation and bacterial abundance, thereby confirming the antibiofilm activity of ulvan. These results correlate with the reduction in EPS production, a key factor responsible for forming biofilms and protecting bacteria from the detrimental effects of antibiotics. Similar reports have also been recorded by Ibrahim et al. (2022), who reported that ulvan derived from green algae, had effectively deterred biofilm formation by *S. agalactiae*, *S. aureus*, *E. faecalis*, *B. subtilis*, *S. epidermidis*, and *L. monocytogenes* strains and further claimed it to be due to electrostatic repulsion between bacteria and carboxylic groups of ulvan possessing negative charge. Mani et al. (2024) reported that fucoidan from brown algae exerted appreciable antibiofilm activity at MIC concentration against *P. vulgaris* and *S. eneterica*, as evidenced by less-dense and disrupted cells under light and fluorescence microscopy. The sulfated polysaccharides from *C. reinhardtii* exhibited dose-dependent antibacterial and antibiofilm effects against *N. mucosa*, *E. coli*, *Streptococcus* spp., and *B. subtilis*. Their action resulted in a 2 to 8-fold reduction in the eDNA content of the EPS compared to the control. This effect is most likely due to the interaction between the sulfated polysaccharides and the EPS, which disrupts the biofilm structure by reducing its density (Vishwakarma and Vavilala, 2019). Results of the present study align with earlier reports indicating that ulvan interrupts with biofilm development through several interconnected mechanisms rather than a single linear pathway. One prominent path is its ability to interfere with EPS production, which is an essential part of bacterial strains to hold together, facilitating initial attachment and serving as a protective barrier against antimicrobials and stress (Gadenne et al., 2015; Barakat et al., 2022). However, by hindering EPS production, ulvan prevents bacteria from establishing the EPS matrix, thereby making them susceptible to external pressures. It has also been reported that ulvan can disrupt quorum sensing (QS), a regulatory mechanism that coordinates adhesion, EPS production and biofilm maturation. Also, altering QS pathways may prevent the production of virulence factors necessary for causing diseases and make them more susceptible to antibiotics (Li et al., 2023). Further, less-dense viable cells in the CLSM images indicate poor adherence and disintegrated architecture, thereby suggesting that ulvan can disrupt bacterial membrane integrity and promote oxidative stress, leading to cell lysis (Sulastri et al., 2021). The promising antibiofilm activity observed in the present study by ulvan against the selected test bacterial pathogens could be attributed to inhibition of EPS, disruption of QS, ROS production and leakage of proteins ultimately destabilizing the biofilm architecture and making the test pathogens more sensitive to environmental challenges and therapeutic agents.

3.6.2.7 *In vitro* antidiabetic activity

Starch-hydrolysing enzymes play a crucial role in the prevention of diabetes, particularly type 2 diabetes, which is caused by insulin resistance. The enzyme inhibitory activity of ulvan was evaluated in comparison to the commercially available drug acarbose, which is known to have side effects. Results showed that with increasing ulvan concentration, enzyme inhibition also increased, reaching a maximum of 73 ± 1.13% at the highest concentration (125 µg/mL), with an IC_{50} of 528.39 µg/mL (Figure 5A). In contrast, acarbose showed a maximum of 95 ± 0.1% at 60 µg/mL (Figure 5B), with an IC_{50} of 12.97 µg/mL (Table 4). Acarbose is associated with well-known side effects, such as abdominal distension, flatulence, meteorism, and diarrhoea, due to its strong inhibitory effect. Koh et al. (2020) inferred that sulfated polysaccharide fucoidan derived from *U. pinnatifida*, exhibited anti-diabetic activities with an IC_{50} of 190 µg/mL. It has been reported that the antidiabetic activity of the polysaccharide depends on the sulfate (%) content and molecular weight of the extracted polysaccharide. In this context, Kim et al. (2015) evidenced that ulvan with 21% sulfate content and a molecular weight of 637 kDa is required for effective α-amylase

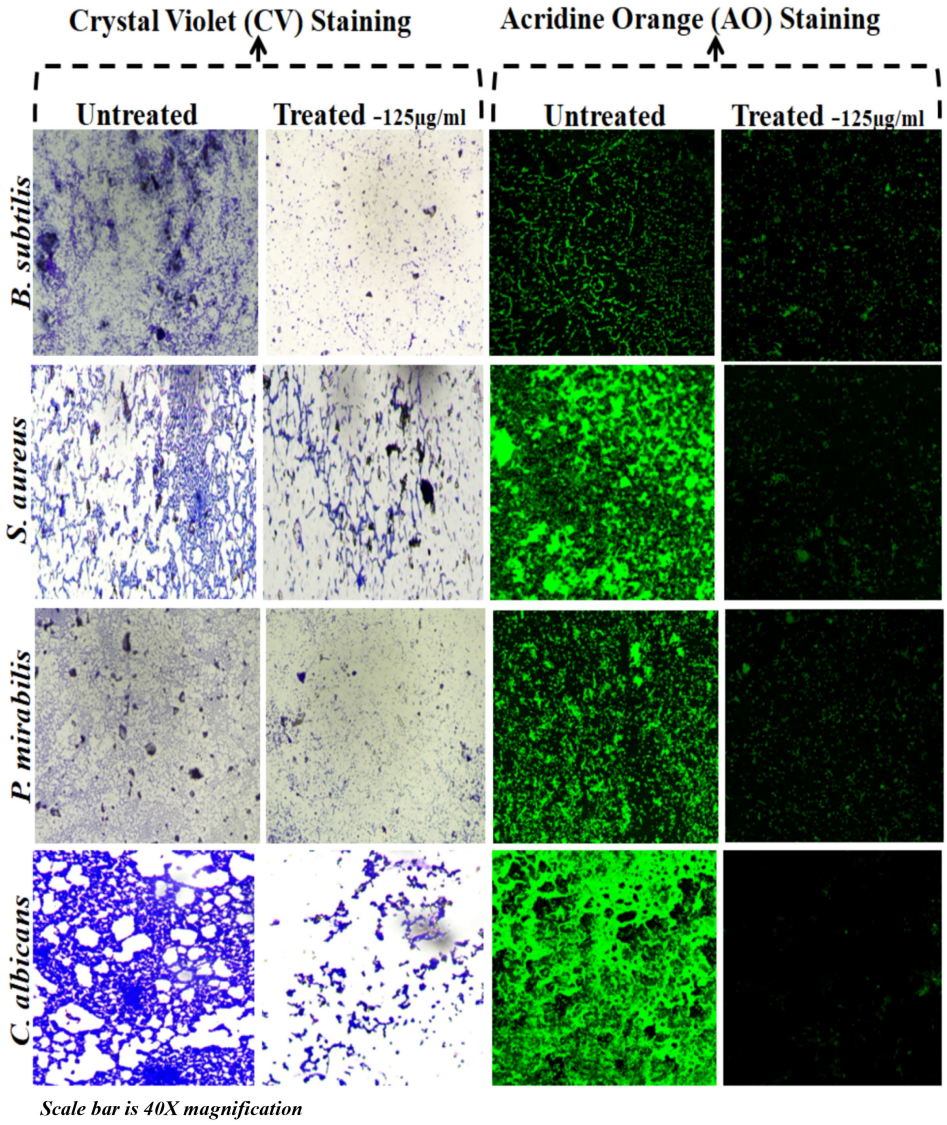


FIGURE 4
Microscopic visualization of biofilm architecture by crystal violet through light microscope (40X) and acridine orange staining through CLSM (200µm). Scale bar is 40X magnification.

inhibition. The α-amylase inhibition of sulfated polysaccharide derived from the edible red alga *Bangiafusco purpurea* was found to be 1260 µg/mL (Jiang et al., 2019). They inferred that carboxylic groups in uronic acid contribute to the inhibition of α-amylase activity. These results emphasize that uronic acid and good sulfate content make the extracted ulvan a potent antidiabetic agent. Previous findings imply that the sulfate content in the seaweed polysaccharides engages electrostatic interactions, hydrogen bonding, and hydrophobic interactions with the positively charged residues at the active and allosteric site of α - amylase enzyme. These interactions significantly cause substantial conformational changes, hinder the formation of enzyme-substrate complex, lead to a non-competitive inhibition and further decrease the efficiency of the enzyme to hydrolyze carbohydrates (Koh et al., 2020; Zhan et al., 2022). Considering the antidiabetic potential of ulvan, the α-amylase enzyme inhibitory activity is comparable to that reported for fucoidan derived from *Padina pavonica* and for alginate derived from *Laminaria digitata* and *Undaria pinnatifida* (Akl et al., 2025; Zaharudin et al., 2018).

3.6.3 Biocompatibility of partially purified ulvan

3.6.3.1 *Artemia* cytotoxicity

The *Artemia* cytotoxicity assay is one of the most convenient assays for determining the toxicity of compounds and toxic substances. In the present study, the mortality rate (%) of *A. salina* nauplii demonstrated a positive relationship with ulvan concentrations, wherein increasing concentrations of ulvan (50 - 200 µg/mL) showed a rise in mortality from 0% to 90% and recorded LC_{50} values of 147.8 µg/mL (Table 4; Figure 6). Supporting the results of present study, *Artemia* cytotoxicity of various polysaccharides

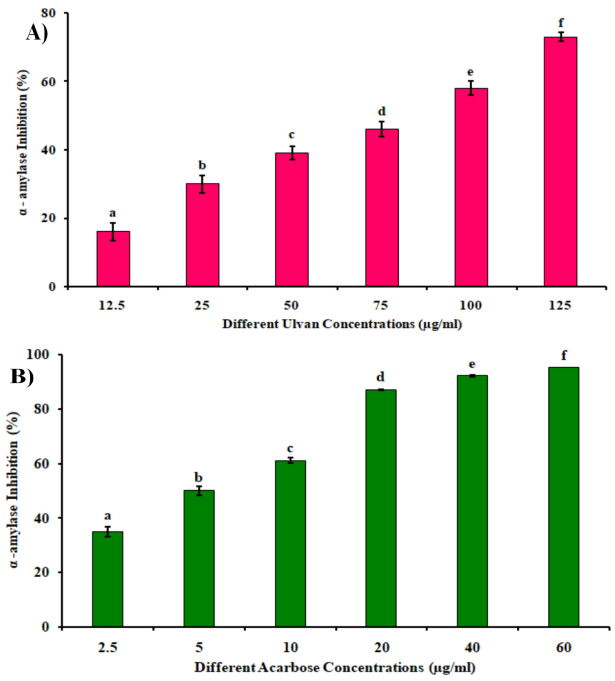


FIGURE 5
α-amylase enzyme inhibitory properties of PP-ulvan **(A)**, and standard drug acarbose **(B)**, Each value is the Mean ± SD of triplicates analysis; each set of bars on **(A)** PP-Ulvan, and **(B)** Acarbose with different superscript (a-f) letters are statistically significant (One-Way ANOVA test: *P* < *0.05*, further, the *post hoc* multiple comparison with SNK test).

derived from *Gracillaria* sp., *Sargassum pallidum*, *Ascophyllum nodosum* demonstrated LC_{50} values ranged between 125 to 140 µg/mL, with mortality in the range of ~5% to >75% (Li et al., 2017). The larvae of Artemia, an invertebrate, are sensitive to a variety of substances and serve as a quick and simple test for predicting the toxicity of natural product extracts and compounds with biological activity (Ntungwe et al., 2020). It is used to detect cytotoxicity, which can be extrapolated to the cells making it a good method to study for new cancer treatments. It has also been proven that the

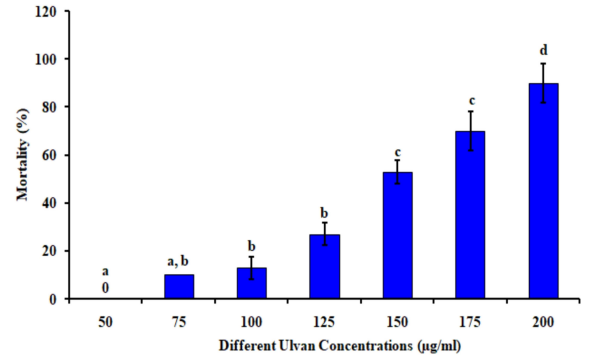


FIGURE 6
Artemia cytotoxicity of PP-ulvan from *U. lactuca* against *A. salina* nauplii. Each value is the mean ± SD of three replicates; bars with different superscript letters are statistically significant (*P* < *0.05*) from percentage response on *Artemia* naupllii in different test concentrations of PP-Ulvan (One-way ANOVA and subsequent *post hoc* multiple comparisons with SNK test).

Artemia lethality assay is comparable with the MTT assay using the mouse fibroblast cell line (L929) (Rajabi et al., 2015). The mechanism underlying Artemia cytotoxicity has been reported to involve visible abnormalities in nauplii treated with plant extracts or bioactive compounds at varying concentrations, after 24 h of exposure. These include improper development of mandibles and underdeveloped endopods, endit, and the swimming setae of the second pair of antennae (Ntungwe et al, 2020).

3.6.4 Cell line cytotoxicity

The cytotoxic activity of ulvan on A431 skin carcinoma cells revealed that at concentrations of 12.5 and 25 µg/mL, cell viability was 96% and 88%, respectively. However, as the concentration increased to 50 µg/mL, the viability decreased to 78% and 60% at 75µg/mL. At the highest concentration (100 µg/mL), the viability dropped to 22%. The negative control (NC) exhibited full cell viability (100%), while the positive control (PC) doxorubicin resulted in 37% viability, confirming its cytotoxic effect (Figures 7A, B). The IC_{50} value of ulvan was calculated to be 82.44 µg/mL (Table 4). These findings suggest that ulvan exhibits a dose-dependent cytotoxic effect on A431 cells, with higher concentrations resulting in a substantial reduction in cell viability. The efficacy of ulvan as an anticancer agent was further evidenced by increased red fluorescence from Ethidium Bromide (EBr) staining, surpassing that of doxorubicin. The abundant, red-stained cells in the treated samples indicate that ulvan disrupts cell viability similar to that of doxorubicin, thus emphasizing that ulvan induces cell death (Figure 7C). In consonance with the results of the present study, previous studies inferred that the polysaccharide ulvan exhibited IC_{50} values ranged between 22.65 and 36.33 µg/mL, against the cell lines such as HepG2, HCT-116, MC7 and HeLa cells, respectively (Ahmed and Ahmed, 2014; Thanh et al., 2016). Previous literature on the mechanism of anticancer activity of ulvan suggests that the presence of monosaccharides, glycosidic linkages, sulfate content, carboxyl and hydroxyl groups present in the ulvan significantly increases the contact between cancer cells, reduces DNA replication, cell proliferation and further results in programmed cell death (Ahmed and Ahmed, 2014; Abd-Ellatef et al., 2017; Usuldin et al., 2021). In the present investigation, the cytotoxicity evaluations were limited to A431 cells as an initial screening strategy. But further evaluation of cytotoxicity against non-cancerous cells is underway and is essential for assessing the therapeutic relevance of ulvan. However, previous studies on the evaluation of the cytotoxicity of ulvan against non-cancerous cells such as keratinocyte (HACAT) and fibroblast (1064sK) recorded the IC_{50} value of 4.2 mg/mL and 1.2 mg/mL, thereby indicating that it requires a higher IC_{50} value to exert cytotoxicity against normal cells (García-Márquez et al., 2023). These results suggest that ulvan is less toxic to normal cells and further substantiate polysaccharide ulvan as a promising source of anticancer agent. Overall, compared with previously reported studies on ulvan from various *Ulva* species, the present investigation demonstrates remarkably high sulfate content, a monosaccharide composition, and pronounced biomedical properties and biocompatibility (Table 6). These differences may be ascribed to variations in environmental factors that

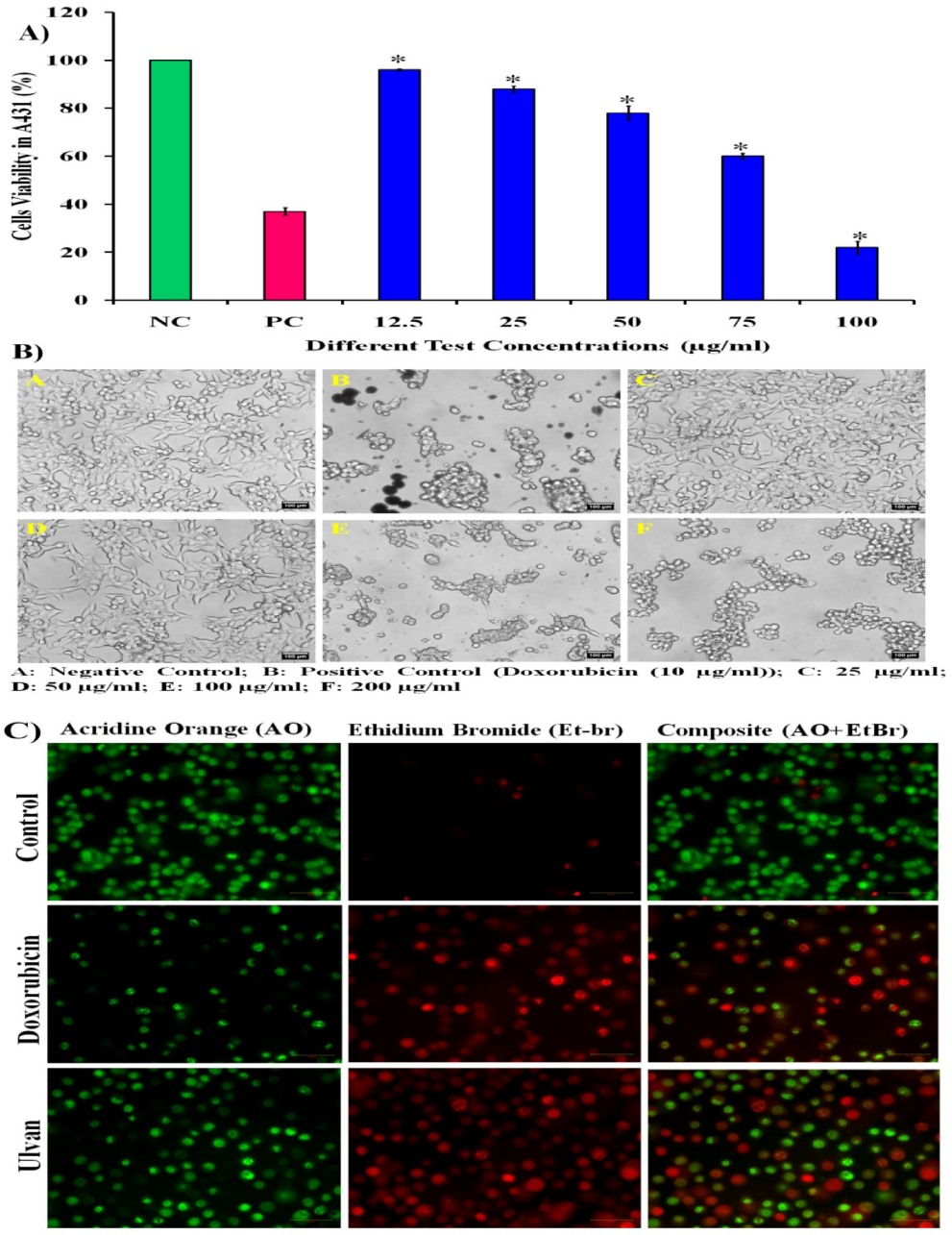


FIGURE 7
Effect of Ulvan on **(A)** MTT cell line cytotoxicity against A431 cells, **(B, C)** showing live and dead cells (scale bar: 200µm). Each value is the Mean ± SD of triplicate analysis. Mean ± SD value indicates a significant percentage response on A431 cell lines, and Positive control as Doxorubicin in different test concentrations of PP-Ulvan compared with negative control in One-way ANOVA, Dunnett test (*P < 0.0001); NS, Non-significant.

influence seaweed growth. Also, such variations significantly alter the physicochemical properties and bioactivity of ulvan.

4 Conclusion

In conclusion, the present study emphasizes that the sulphated polysaccharide ulvan derived from *U. lactuca* exhibits promising *in vitro* antibacterial and antibiofilm activity, which suggests ulvan holds significant promise as a multifunctional biomaterial for applications in wound healing and implant coatings and advanced biomedical systems. The free-radical-scavenging properties of ulvan underscore its protective role against oxidative stress, while its cytotoxicity against A431 cells strongly suggests its potential as an antiproliferative agent. The sensory and structural characteristics of the ulvan were clearly confirmed by a series of organoleptic and spectroscopic analysis. Notably, the integrated evaluation of anti-biofilm efficacy and cytotoxic activity against A431 cells represents an unexplored aspect, highlighting the novelty of this study. Collectively, the findings of the present study suggest that ulvan is a potent bioactive polysaccharide with

TABLE 6 Comparative evaluation of ulvan and its biomedicinal properties (2015–2025) with emphasis on current investigation.

Seaweed species	Extraction methods	%		Monosaccharides composition	Biomedicinal properties.				Toxicity		References
		Sulfate content	Uronic acid content		Antioxidant	Antimicrobial	Antibiofilm	Amylase inhibition	Hemolysis	*Artemia*/cell line cytotoxicity	
Ulva fertusa	Acid with water extraction	19.7%	23.8%	Glucuronic acid, Idulonic acid, Rhamnose, Xylose,	NR	NR	NR	NR	NR	NR	Tako et al, 2015
Ulva lactuca	Hot water extraction	18.9%	21.5%	Rhamnose, Galactose, Xylose, Manose, Glucose	NR	NR	NR	NR	NR	Hepato cellular carcinoma, Human breast cancer, Cervical cancer	Thanh et al, 2016
Ulva lactuca	Acid with combined in enzymatic and chemical extraction	NR	NR	Uronic acid, Rhamnose, Xylose, Mannose, Galactose and Arabinose	Total antioxidant ability, DPPH, reducing power assay, metal chelating assay	NR	NR	NR	NR	NR	Yaich et al, 2017
Ulva fasciata Delile	Water extraction	20.45%	NR	Rhamnose, pyranose, fucose, arabinose, mannose,	DPPH	Antibacterial and Antifungal	NR	NR	NR	NR	Barakat et al, 2022
Ulva rigida	Hot water extraction	NR	NR	Rhamnose, Glucuronic acid, and Xylose	NR	NR	NR	NR	NR	1064sk, HACAT, U-937, G-361, HCT-116	García-Márquez et al, 2023
Ulva lactuca Linnaeus	Hot water extraction	NR	2.23%	Fructose, Glucose, Rhamnose, Galactose, Melibiose	DPPH, FRAP	Antibacterial	NR	NR	NR	Vero cells, PC-3 and A-549 cell lines,	Maray et al, 2023
Ulva lactuca	ultrasound-assisted extraction (UAE)	NR	NR	Rhamnose, Glucose, Glucuronic acid, Xylose, Iduronic Acid	ROS	NR	NR	NR	NR	THP1	Cameselle et al, 2025
Ulva intestinalis	Hot water extraction	17.18%	NR	Galactose, Mannose, Xylose	DPPH, ABTS, Total Anti-oxidant potential, FRAP, HPO	Antibacterial	NR	NR	NR	NR	Kamali et al, 2025
Ulva lactuca	Hot water extraction	20.1%	19.03%	Rhamnose, galactose, glucose, fructose, arabinose, and fucose	DPPH, FRAP, HPO, TAA	Antibacterial and Antifungal	CV stained 96 well plate, EPS, Protein leakage, ROS effects and CLSM	Porcine pancreatic amylase	NR	*Artemia* naupllii and A431 cells line (Skin cancer Line)	Current Study

NR, No Research.

10.3389/fmars.2026.1817180

promising pharmaceutical potential; nevertheless, further *in vivo* and clinical studies are necessary to validate its therapeutic applicability.

Data availability statement

The raw data supporting the conclusions of this article will be made available by the authors, without undue reservation.

Ethics statement

Ethical approval was not required for the studies on humans in accordance with the local legislation and institutional requirements because only commercially available established cell lines were used. Ethical approval was not required for the studies on animals in accordance with the local legislation and institutional requirements because only commercially available established cell lines were used.

Author contributions

SM: Writing – original draft, Investigation, Visualization, Conceptualization. RR: Validation, Data curation, Writing – review & editing, Resources. TD: Data curation, Methodology, Investigation, Formal analysis, Writing – review & editing. SB: Writing – review & editing, Formal analysis, Methodology, Validation. GR: Data curation, Methodology, Validation, Writing – original draft. EK: Conceptualization, Methodology, Investigation, Formal analysis, Writing – review & editing. GI: Data curation, Writing – review & editing, Validation, Methodology. CA: Data curation, Validation, Writing – review & editing, Formal analysis. SP: Investigation, Conceptualization, Supervision, Writing – review & editing, Project administration.

Funding

The author(s) declared that financial support was received for this work and/or its publication. The corresponding author (S. Prakash) gratefully acknowledge the financial assistance supported in the form of Chief Minister's Research Grant (CMRG), Directorate of Technical Education (DoTE), Chennai, Tamil Nadu (Project ID: CMRG25-UE-0026).

Acknowledgments

The authors are grateful to acknowledged in Dr. J. Jayalalithaa Fisheries University, Nagapattinum and the Nanotechnology Research Centre (NRC), SRM Institute of Science and Technology, and Saveetha Institute of Medical and Technical Sciences (SIMATS), Saveetha University for providing the necessary facilities to carry out the research work.

Conflict of interest

The author(s) declared that this work was conducted in the absence of any commercial or financial relationships that could be construed as a potential conflict of interest.

The author SP declared that they were an editorial board member of Frontiers, at the time of submission. This had no impact on the peer review process and the final decision.

Generative AI statement

The author(s) declared that generative AI was not used in the creation of this manuscript.

Any alternative text (alt text) provided alongside figures in this article has been generated by Frontiers with the support of artificial intelligence and reasonable efforts have been made to ensure accuracy, including review by the authors wherever possible. If you identify any issues, please contact us.

Publisher's note

All claims expressed in this article are solely those of the authors and do not necessarily represent those of their affiliated organizations, or those of the publisher, the editors and the reviewers. Any product that may be evaluated in this article, or claim that may be made by its manufacturer, is not guaranteed or endorsed by the publisher.

Supplementary material

The Supplementary Material for this article can be found online at: https://www.frontiersin.org/articles/10.3389/fmars.2026.1817180/full#supplementary-material

References

Abd-Ellatef, G. F., Ahmed, O. M., Abdel-Reheim, E. S., and Abdel-Hamid, A. Z. (2017). Ulva lactuca polysaccharides prevent Wistar rat breast carcinogenesis through the augmentation of apoptosis, enhancement of antioxidant defense system, and suppression of inflammation. *Breast Cancer* 9, 67–83. doi: 10.2147/bctt.s125165

Abu-Resha, A. M., El-Sheekh, M. M., Abou-El-Souod, G. W., Morsi, H., and Makhlof, M. (2026). Optimized production and characterization of ulvan from Ulva lactuca with *in vitro* biological activities. *Sci. Rep.* 16, 11374. doi: 10.1038/s41598-026-44503-7

Adrien, A., Bonnet, A., Dufour, D., Baudouin, S., Maugard, T., and Bridiau, N. (2019). Anticoagulant activity of sulfated ulvan isolated from the green macroalga Ulva rigida. *Mar. Drugs* 17, 291. doi: 10.3390/md17050291

Ahmed, O. M., and Ahmed, R. R. (2014). Anti-proliferative and apoptotic efficacies of ulvan polysaccharides against different types of carcinoma cells *in vitro* and *in vivo*. *J. Cancer Sci. Ther.* 6, 202–208. doi: 10.4172/1948-5956.1000272

Akl, F. M., El-Sheekh, M. M., Makhlof, M. E., and Ahmed, S. I. (2025). Antimicrobial, antidiabetic, antiviral, and antioxidant activities of fucoidan extracted from the brown seaweed Padina pavonica. *BMC Biotech.* 25, 70. doi: 10.1186/s12896-025-01004-1

Akter, A., Sobuj, M. K. A., Islam, M. S., Chakroborty, K., Tasnim, N., Ayon, M. H., et al. (2024). Seaweed polysaccharides: Sources, structure and biomedical applications with special emphasis on antiviral potentials. *Future Foods.* 10, 100440. doi: 10.1016/j.fufo.2024.100440

Alfinaikh, R. S., Alamry, K. A., and Hussein, M. A. (2025). Sustainable and biocompatible hybrid materials-based sulfated polysaccharides for biomedical applications: a review. *RSC. Adv.* 15, 4708–4767. doi: 10.1039/d4ra07277d

Alves, A., Sousa, R. A., and Reis, R. L. (2013). A practical perspective on ulvan extracted from green algae. *J. Appl. Phycol.* 25, 407–424. doi: 10.1007/s10811-012-9875-4

Anisha, G. S., Augustianath, T., Padmakumari, S., Singhania, R. R., Pandey, A., and Patel, A. K. (2023). Ulvan from green macroalgae: Bioactive properties advancing tissue engineering, drug delivery systems, food industry, agriculture and water treatment. *Bioresour. Technol. Rep.* 22, 101457. doi: 10.1016/j.biteb.2023.101457

Anjali, R., Palanisamy, S., Vinosha, M., Selvi, A. M., Manikandakrishnan, M., Sathiyaraj, G., et al. (2022). Sulfated polysaccharides from Caulerpa sertularioides: Extraction and evaluation of antioxidant, antibacterial, and immunological properties. *Ind. Crops Prod.* 188, 115671. doi: 10.1016/j.indcrop.2022.115671

AOAC (2005). *Official Methods of Analysis. 18th edn* (Arlington, VA, USA: Association of Official Analytical Chemists).

Ayrapetyan, O. N., Obluchinskaya, E. D., Zhurishkina, E. V., Skorik, Y. A., Lebedev, D. V., Kulminskaya, A. A., et al. (2021). Antibacterial properties of fucoidans from the brown algae Fucus vesiculosus L. of the Barents Sea. *Biology* 10, 67. doi: 10.3390/biology10010067

Barakat, K. M., Ismail, M. M., Abou El Hassayeb, H. E., El Sersy, N. A., and Elshobary, M. E. (2022). Chemical characterization and biological activities of ulvan extracted from Ulva fasciata (Chlorophyta). *Rend. Lincei. Sci. Fis. Nat.* 33, 829–841. doi: 10.1007/s12210-022-01103-7

Becerra, M. C., Eraso, A. J., and Albesa, I. (2003). Comparison of oxidative stress induced by ciprofloxacin and pyoverdin in bacteria and in leukocytes to evaluate toxicity. *Luminescence.: J. Biol. Chem. Luminescence.* 18, 334–340. doi: 10.1002/bio.742

Behzadnia, A., Moosavi-Nasab, M., and Oliyaei, N. (2024). Anti-biofilm activity of marine algae-derived bioactive compounds. *Front. Microbiol.* 15, 270174. doi: 10.3389/fmicb.2024.1270174

Benito-González, I., Gökşen, G., Pérez-Bassart, Z., López-Rubio, A., Sánchez, R., Alonso, J. M., et al. (2021). Pilot plant scale-up of the production of optimized starch-based biocomposites loaded with cellulosic nanocrystals from Posidonia oceanica waste biomass. *Food Packag. Shelf. Life* 30, 100730. doi: 10.1016/j.fpsl.2021.100730

Bjarnsholt, T., Buhlin, K., Dufrêne, Y. F., Gomelsky, M., Moroni, A., Ramstedt, M., et al. (2018). Biofilm formation–what we can learn from recent developments. *J. Internal Med.* 284, 332–345. doi: 10.1111/joim.12782

Cameselle, C., Maietta, I., Torres, M. D., Simón-Vázquez, R., and Domínguez, H. (2025). Optimization of ultrasound-assisted extraction of bioactive compounds and biopolymers from Ulva spp. using response surface methodology. *J. Appl. Phycol.* 37, 2031–2050. doi: 10.1007/s10811-025-03492-2

Ciancia, M., Quintana, I., Vizcargüénaga, M. I., Kasulin, L., de Dios, A., Estevez, J. M., et al. (2007). Polysaccharides from the green seaweeds Codium fragile and C. vermilara with controversial effects on hemostasis. *Int. J. Biol. Macromol.* 41, 641–649. doi: 10.1016/j.ijbiomac.2007.08.007

CLSI (Clinical and Laboratory Standards Institute) (2015). *Methods for Dilution Antimicrobial Susceptibility Tests for Bacteria that Grow Aerobically* (Wayne, PA: CLSI). Approved Standard-Tenth Edition (M07-A10).

Costa, C., Alves, A., Pinto, P. R., Sousa, R. A., da Silva, E. A. B., Reis, R. L., et al. (2012). Characterization of ulvan extracts to assess the effect of different steps in the extraction procedure. *Carbohydr. Polym.* 88, 537–546. doi: 10.1016/j.carbpol.2011.12.041

Costa, L. S., Fidelis, G. P., Cordeiro, S. L., Oliveira, R. M., Sabry, D. A., Câmara, R. B. G., et al. (2010). Biological activities of sulfated polysaccharides from tropical seaweeds. *Biomed. Pharmacother.* 64, 21–28. doi: 10.1016/j.biopha.2009.03.005

Digala, P., Saravanan, M., Dhanraj, M., Pamarthi, J., Muralidharan, S., Narikimelli, A., et al. (2022). Optimized extraction of sulfated polysaccharide from brown seaweed Sargassum polycystum and its evaluation for anti-cancer and wound healing potential. *S. Afr. J. Bot.* 151, 345–359. doi: 10.1016/j.sajb.2022.03.015

Divya, D., Madhuri, K., Kumar, R., Kannan, K., Jeyameenakshi, A., Karthick Rajan, D., et al. (2021). Antibacterial and cytotoxicity activities of biosynthesized silver oxide (Ag2O) nanoparticles using Bacillus paramycoides. *J. Drug Delivery. Sci. Technol.* 61, 102111. doi: 10.1016/j.jddst.2020.102111

Durgadevi, R., Abirami, G., Alexpandi, R., Nandhini, K., Kumar, P., Prakash, S., et al. (2019). Explication of the potential of 2-hydroxy-4-methoxybenzaldehyde in hampering uropathogenic Proteus mirabilis crystalline biofilm and virulence. *Front. Microbiol.* 10, 2804. doi: 10.3389/fmicb.2019.02804

Farsimadan, M., and Motamedifar, M. (2021). The effects of human immunodeficiency virus, human papillomavirus, herpes simplex virus-1 and-2, human herpesvirus-6 and-8, cytomegalovirus, and hepatitis B and C virus on female fertility and pregnancy. *Br. J. Biomed. Sci.* 78, 1–11. doi: 10.1080/09674845.2020.1803540

Figueira, T. A., Da Silva, A. J. R., Prast, A. E., Valentin, Y. Y., and Oliveira, V. P. (2020). Structural characterization of ulvan polysaccharide from cultivated and collected Ulva fasciata (Chlorophyta). *Adv. Biosci. Biotechnol.* 11, 206–216. doi: 10.4236/abb.2020.115016

Filisetti-Cozzi, T. M. C. C., Nicholas, C., and Carpita, N. C. (1991). Measurement of uronic acids without interference from neutral sugars. *Anal. Biochem.* 197, 157–162. doi: 10.1016/0003-2697(91)90372-z

Gadenne, V., Lebrun, L., Jouenne, T., and Thebault, P. (2015). Role of molecular properties of ulvans on their ability to elaborate antiadhesive surfaces. *J. Biomed. Mater. Res. Part A.* 103, 1021–1028. doi: 10.1002/jbm.a.35245

Gao, X., Qu, H., Shan, S., Song, C., Baranenko, D., Li, Y., et al. (2020). A novel polysaccharide isolated from Ulva Pertusa: Structure and physicochemical property. *Carbohydr. Polym.* 233, 115849. doi: 10.1016/j.carbpol.2020.115849

García-Márquez, J., Moreira, B. R., Valverde-Guillén, P., Latorre-Redoli, S., Caneda-Santiago, C. T., Acién, G., et al. (2023). *In vitro* and *in vivo* effects of ulvan polysaccharides from Ulva rigida. *Pharmaceuticals* 16, 660. doi: 10.1016/j.bcdf.2014.01.002

Gonzales, K. N., Torres, F. G., Carsí, M., and Sanchis, M. J. (2025a). Effects of morphology and extraction procedures on the chemical, thermal and dielectric properties of ulvan polysaccharides. *Int. J. Biol. Macromol.* 321, 146121. doi: 10.1016/j.ijbiomac.2025.146121

Gonzales, K. N., Troncoso, O. P., and Torres, F. G. (2025b). Controlled extraction and characterization of ulvan from Ulva papenfussii with potential applications in sustainable energy. *J. Appl. Phycol.* 37, 2051–2059. doi: 10.1007/s10811-025-03503-2

Guidara, M., Yaich, H., Amor, I. B., Fakhfakh, J., Gargouri, J., Lassoued, S., et al. (2021). Effect of extraction procedures on the chemical structure, antitumor and anticoagulant properties of ulvan from Ulva lactuca of Tunisia coast. *Carbohydr. Polym.* 253, 117283. doi: 10.1016/j.carbpol.2020.117283

Guidara, M., Yaich, H., Petrut, R., Richel, A., Blecker, C., Attia, H., et al. (2024). Manufacturing bioprocess of novel cream formulations based on polysaccharides "ulvans" from green seaweed Ulva lactuca: Effect of extraction procedures and concentrations on the optical and rheological properties of ulvan creams. *Sustain. Chem. Pharm.* 42, 101852. doi: 10.1016/j.scp.2024.101852

Hale, J., Furch, A., Gerhäuser, J., Gaukel, V., and Wefers, D. (2024). Ice recrystallization inhibition activity of chemically defined carrageenans. *Food Hydrocolloids.* 157, 110423. doi: 10.1016/j.foodhyd.2024.110423

Hedge, J. E., and Hofreiter, B. T. (1962). Methods of estimating starch and carbohydrates. *Carbohydr. Chem.* 17, 163–201. doi: 10.4236/as.2013.49B009

Hou, L., Liu, Z., Zhang, D., Liu, S., Chen, Z., Wu, Q., et al. (2024). BR regulates wheat root salt tolerance by maintaining ROS homeostasis. *Planta* 260, 5. doi: 10.1007/s00425-024-04429-8

Ibrahim, M. I., Amer, M. S., Ibrahim, H. A., and Zaghloul, E. H. (2022). Considerable production of ulvan from Ulva lactuca with special emphasis on its antimicrobial and antifouling properties. *Appl. Biochem. Biotechnol.* 194, 3097–3118. doi: 10.1007/s12010-022-03867-y

Jayawardena, T. U., Wang, L., Sanjeewa, K. A., Kang, S. I., Lee, J. S., and Jeon, Y. J. (2020). Antioxidant potential of sulfated polysaccharides from Padina boryana; Protective effect against oxidative stress in *in vitro* and *in vivo* zebrafish model. *Mar. Drugs* 18, 212. doi: 10.3390/md18040212

Jeesha, S., Revathi, D., Ganapathy, D., and Ramasubburayan, R. (2024). Bioinspired green synthesis of ZnO nanoparticles by marine-derived Streptomyces plicatus and its multifaceted biomedicinal properties. *Microb. Pathogen.* 193, 106758. doi: 10.1016/j.micpath.2024.106758

Jeyachandran, S., and Aman, M. (2025). Valorization of fish scales and bones: a sustainable source of bioactive proteins and collagen for nutraceuticals. *Bioresour. Bioprocess.* 12, 141. doi: 10.1186/s40643-025-00970-w

Jiang, Z., Yu, G., Liang, Y., Song, T., Zhu, Y., Ni, H., et al. (2019). Inhibitory effects of a sulfated polysaccharide isolated from edible red alga Bangiafusco purpurea on α amylase and α-glucosidase. *Biosci. Biotechnol. Biochem.* 83, 2065–2074. doi: 10.1080/09168451.2019.1634515

Jiao, G., Yu, G., Zhang, J., and Ewart, H. S. (2011). Chemical structures and bioactivities of sulfated polysaccharides from marine algae. *Mar. Drugs* 9, 196–223. doi: 10.3390/md9020196

Jun, J. Y., Jung, M. J., Jeong, I. H., Yamazaki, K., Kawai, Y., and Kim, B. M. (2018). Antimicrobial and antibiofilm activities of sulfated polysaccharides from marine algae against dental plaque bacteria. *Mar. Drugs* 16, 301. doi: 10.3390/md16090301

Kamali, M., Shabanpour, B., Pourashouri, P., and Kordjazi, M. (2025). Ulvan from Ulva intestinalis of the Caspian Sea: Characteristics, antioxidant, and antibacterial activities. *Carbohydr. Polym. Technol. Appl.* 11, 100872. doi: 10.1016/j.carpta.2025.100872

Kang, M. G., Khan, F., Jo, D. M., Oh, D., Tabassum, N., and Kim, Y. M. (2022). Antibiofilm and antivirulence activities of gold and zinc oxide nanoparticles synthesized from Kimchi-isolated Leuconostoc sp. strain C2. *Antibiotics* 11, 1524. doi: 10.3390/antibiotics11111524

Kazemi, M., Fathi, M., Jahanbin, K., Taghdir, M., and Abbaszadeh, S. (2023). Optimization of ultrasonic-assisted hot acidic solvent extraction of ulvan from Ulva intestinalis of the Persian Gulf: Evaluation of structural, techno-functional, and bioactivity properties. *Food Hydrocolloids.* 142, 108837. doi: 10.1016/j.foodhyd.2023.108837

Kemp, W. (1991). "Infrared spectroscopy," in *Organic Spectroscopy*. Ed. W. Kemp (The Macmillan Press Ltd, Hong Kong (ELBS edition). third ed.

Khaerunnisa, M., Arfah, R. A., and Permatasari, N. U. (2024). "Isolation of sulfate polysaccharides (Ulvan) from the green algae of Ulva lactuca and characterization of its functional groups", in: *AIP Conference Proceedings* (AIP Publishing), 2774. 030006. doi: 10.1063/5.0167182

Kidgell, J. T., Magnusson, M., de Nys, R., and Glasson, C. R. (2019). Ulvan: a systematic review of extraction, composition and function. *Algal. Res.* 39, 101422. doi: 10.1016/j.algal.2019.101422

Kim, J. K., Cho, M. L., Karnjanapratum, S., Shin, I. S., and You, S. G. (2011). *In vitro* and *in vivo* immunomodulatory activity of sulfated polysaccharides from Enteromorpha prolifera. *Int. J. Biol. Macromol.* 49, 1051–1058. doi: 10.1016/j.ijbiomac.2011.08.032

Kim, K. T., Rioux, L. E., and Turgeon, S. L. (2015). Molecular weight and sulfate content modulate the inhibition of α-amylase by fucoidan relevant for type 2 diabetes management. *PharmaNutrition* 3, 108–114. doi: 10.1016/j.phanu.2015.02.001

Kim, D. E., Shin, J., Kim, H. J., and Kim, H. J. (2025). Valorization of the invasive alga Ulva australis: impact of solvent extraction methods on bioactive compounds and antioxidant potential. doi: 10.2139/ssrn.5561185. Available online at SSRN 5561185.

Koh, H. S. A., Lu, J., and Zhou, W. (2020). Structural dependence of sulfated polysaccharide for diabetes management: fucoidan from Undaria pinnatifida inhibiting α-glucosidase more strongly than α-amylase and amyloglucosidase. *Front. Pharmacol.* 11, 831. doi: 10.3389/fphar.2020.00831

Kostas, E. T., Adams, J. M. M., Ruíz, H. A., Durán-Jiménez, G., and Lye, G. J. (2021). Macroalgal biorefinery concepts for the circular bioeconomy: a review on biotechnological developments and future perspectives. *Renewable Sustain. Energy Rev.* 151, 111553. doi: 10.1016/j.rser.2021.111553

Kraiem, M., Ben Hamouda, S., Eleroui, M., Ajala, M., Feki, A., Dghim, A., et al. (2024). Anti-inflammatory and immunomodulatory properties of a crude polysaccharide derived from green seaweed Halimeda tuna: computational and experimental evidences. *Mar. Drugs* 22, 85. doi: 10.3390/md22020085

Lahaye, M., and Robic, A. (2007). Structure and functional properties of ulvan, a polysaccharide from green seaweeds. *Biomacromolecules* 8, 1765–1774. doi: 10.1021/bm061185q

Li, C., Tang, T., Du, Y., Jiang, L., Yao, Z., Ning, L., et al. (2023). Ulvan and Ulva oligosaccharides: a systematic review of structure, preparation, biological activities and applications. *Bioresour. Bioprocess.* 10, 66. doi: 10.1186/s40643-023-00690-z

Li, X., Xiong, F., Liu, Y., Liu, F., Hao, Z., and Chen, H. (2018). Total fractionation and characterization of the water-soluble polysaccharides isolated from Enteromorpha intestinalis. *Int. J. Biol. Macromol.* 111, 319–325. doi: 10.1016/j.ijbiomac.2018.01.018

Li, C. Y., Zhang, R. Q., Fu, K. Y., Li, C., and Li, C. (2017). Effects of high temperature on starch morphology and the expression of genes related to starch biosynthesis and degradation. *J. Cereal Sci.* 73, 25–32. doi: 10.1016/j.jcs.2016.11.005

Liu, M., Liu, Y., Cao, M. J., Liu, G. M., Chen, Q., Sun, L., et al. (2017). Antibacterial activity and mechanisms of depolymerized fucoidans isolated from Laminaria japonica. *Carbohydr. Polym.* 172, 294–305. doi: 10.1016/j.carbpol.2017.05.060

Lowry, O. H., Rosebrough, N. J., Farr, A. L., and Randall, R. J. (1951). Protein measurement with the Folin phenol reagent. *J. Biol. Chem.* 193, 265–275. doi: 10.1016/s0021-9258(19)52451-6

Lucien, B. V., Douglas, M. H., Scott, P. M., John, K. H., and Michael, J. M. (2023). Antimicrobial susceptibility testing to evaluate minimum inhibitory concentration values of clinically relevant antibiotics. *STAR Protocols* 4 (3), 102512. doi: 10.1016/j.xpro.2023.102512

Mani, G., Rajendran, I., Jayakumar, T., Mani, A., Govindaraju, R., and Dhayalan, S. (2024). Evaluation of antibiofilm and antiquorum sensing activities of fucoidan characterized from Padina boryana against nosocomial pathogens. *Appl. Biochem. Biotechnol.* 196, 4727–4744. doi: 10.1007/s12010-025-05383-1

Maray, S. O., Abdel-Kareem, M. S., Mabrouk, M. E., El-Halmouch, Y., and Makhlof, M. E. (2023). *In vitro* assessment of antiviral, antimicrobial, antioxidant and anticancer activities of ulvan extracted from the green seaweed Ulva lactuca. *Thalassas.: An. Int. J. Mar. Sci.* 39, 779–790. doi: 10.1007/s41208-023-00584-z

McFarland, J. (1907). The Nephelometer: an instrument for estimating the number of bacteria in suspensions used for calculating the opsonic index and for vaccines. *J. Am. Med. Assoc.* 49, 1176–1178. doi: 10.1001/jama.1907.25320140022001f

Moawad, M. N., El-Sayed, A. A., Abd El Latif, H. H., El-Naggar, N. A., El-Din, N. G. S., and Tadros, H. R. (2022). Chemical characterization and biochemical activity of polysaccharides isolated from Egyptian Ulva fasciata Delile. *Oceanologia* 64, 117–130. doi: 10.1016/j.oceano.2021.09.008

Negreanu-Pirjol, B. S., Negreanu-Pirjol, T., Popoviciu, D. R., Anton, R. E., and Prelipcean, A. M. (2022). Marine bioactive compounds derived from macroalgae as new potential players in drug delivery systems: a review. *Pharmaceutics* 14, 1781. doi: 10.3390/pharmaceutics14091781

Ntungwe, N. E., Domínguez-Martín, E. M., Roberto, A., Tavares, J., Isca, V., Pereira, P., et al. (2020). Artemia species: an important tool to screen general toxicity samples. *Curr. Pharm. Des.* 26, 2892–2908. doi: 10.2174/1381612826666200406083035

Ogunyemi, O. M., Gyebi, G. A., Saheed, A., Paul, J., Nwaneri-Chidozie, V., Olorundare, O., et al. (2022). Inhibition mechanism of alpha-amylase, a diabetes target, by a steroidal pregnane and pregnane glycosides derived from Gongronema latifolium Benth. *Front. Mol. Biosci.* 9, 866719. doi: 10.3389/fmolb.2022.866719

Palanisamy, S., Vinosha, M., Marudhupandi, T., Rajasekar, P., and Prabhu, N. M. (2017). *In vitro* antioxidant and antibacterial activity of sulfated polysaccharides isolated from Spatoglossum asperum. *Carbohydr. Polym.* 170, 296–304. doi: 10.1016/j.carbpol.2017.04.085

Pari, R. F., Uju, U., Hardiningtyas, S. D., Ramadhan, W., Wakabayashi, R., Goto, M., et al. (2025). Ulva seaweed-derived ulvan: a promising marine polysaccharide as a sustainable resource for biomaterial design. *Mar. Drugs* 23, 56. doi: 10.3390/md23020056

Patil, U., Saetang, J., Zhang, B., Kim, JT., and Benjakul, S. (2025). Physicochemical properties, *in vitro* digestion and absorption of bio-calcium powders derived from Asian seabass gills as affected by bleaching treatment. *Food Chem.* 497, 147080. doi: 10.1016/j.foodchem.2025.147080

Powell, L. C., Pritchard, M. F., Ferguson, E. L., Powell, K. A., Patel, S. U., Rye, P. D., et al. (2018). Targeted disruption of the extracellular polymeric network of Pseudomonas aeruginosa biofilms by alginate oligosaccharides. *NPJ Biofilms. Microbiomes.* 4, 13. doi: 10.1038/s41522-018-0056-3

Prakash, S., Pattukumar, V., Thirumurugan, D., Saravanan, R., Singh, R. R., Immanuel, G., et al. (2023). Exploring biotechnological approaches on *in vitro* callus induction and evaluation of biomedicinal properties of Cleome gynandra L. *Process. Biochem.* 134, 316–328. doi: 10.1016/j.procbio.2023.10.011

Prakash, S., Ramasubburayan, R., Iyapparaj, P., Arthi, A. P. R., Ahila, N. K., Ramkumar, V. S., et al. (2015). Environmentally benign antifouling potentials of triterpene-glycosides from Streptomyces fradiae: a mangrove isolate. *RSC. Adv.* 5, 29524–29534. doi: 10.1039/c4ra15335a

Prakash, S., Ramasubburayan, R., Ramkumar, V. S., Kannapiran, E., Palavesam, A., and Immanuel, G. (2016). *In vitro* scientific evaluation on antimicrobial, antioxidant, cytotoxic properties and phytochemical constituents of traditional coastal medicinal plants. *Biomed. Pharmacother.* 83, 648–657. doi: 10.1016/j.biopha.2016.07.019

Pramanik, S., Singh, A., Abualsoud, B. M., Deepak, A., Nainwal, P., Sargsyan, A. S., et al. (2024). From algae to advancements: laminarin in biomedicine. *RSC. Adv.* 14, 3209–3231. doi: 10.1039/d3ra08161c

Qi, H., Zhao, T., Zhang, Q., Li, Z., Zhao, Z., and Xing, R. (2005). Antioxidant activity of different molecular weight sulfated polysaccharides from Ulva pertusa Kjellm (Chlorophyta). *J. Appl. Phycol.* 17, 527–534. doi: 10.1007/s10811-005-9003-9

Qin, L., Yang, Y., and Mao, W. (2023). Anticoagulant property of a sulfated polysaccharide with unique structural characteristics from the green alga Chaetomorpha aerea. *Mar. Drugs* 21, 88. doi: 10.3390/md21020088

Rahimi, F., Tabarsa, M., and Rezaei, M. (2016). Ulvan from green algae Ulva intestinalis: optimization of ultrasound-assisted extraction and antioxidant activity. *J. Appl. Phycol.* 28, 2979–2990. doi: 10.1007/s10811-016-0824-5

Rajabi, S., Ramazani, A., Hamidi, M., and Naji, T. (2015). Artemia salina as a model organism in toxicity assessment of nanoparticles. *DARU. J. Pharm. Sci.* 23, 20. doi: 10.1186/s40199-015-0105-x

Rajasekar, P., Palanisamy, S., Anjali, R., Vinosha, M., Elakkiya, M., Marudhupandi, T., et al. (2019). Isolation and structural characterization of sulfated polysaccharide from Spirulina platensis and its bioactive potential: *in vitro* antioxidant, antibacterial activity and zebrafish growth and reproductive performance. *Int. J. Biol. Macromol.* 141, 809–821. doi: 10.1016/j.ijbiomac.2019.09.024

Rajasekaran, J., and Viswanathan, P. (2023). Anti-bacterial and antibiofilm properties of seaweed polysaccharide-based nanoparticles. *Aquat. Int.* 31, 2799–2823. doi: 10.1007/s10499-023-01111-w

Rajivgandhi, G. N., Kanisha, C. C., Ramachandran, G., Manoharan, N., Mothana, R. A., Siddiqui, N. A., et al. (2021). Phytochemical screening and anti-oxidant activity of Sargassum wightii enhances the anti-bacterial activity against Pseudomonas aeruginosa. *Saudi. J. Biol. Sci.* 28, 1763. doi: 10.1016/j.sjbs.2020.12.018

Ramasubburayan, R., Senthilkumar, N., Kanagaraj, K., Basumatary, S., Kathiresan, S., Manjunathan, J., et al. (2023). Environmentally benign, bright luminescent carbon dots from IV bag waste and chitosan for antimicrobial and bioimaging applications. *Environ. Res.* 238, 117182. doi: 10.1016/j.envres.2023.117182

Ravi, C., Manogaran, Y., and Ramasamy, P. (2025). Extraction, characterization and antioxidative potential of a bioactive polymeric material from the cuttlebone of Sepia brevimana. *Texila. Int. J. Public Health* 13, 69. doi: 10.21522/TIJPH.2013.13.01.Art069

Rempfert, K. R., Bell, S., Kasanke, C. P., Zhao, Q., Zhao, X., Lipton, A., et al. (2024). Biomolecular budget of persistent, microbial-derived soil organic carbon: the importance of underexplored pools. *Sci. Total. Environ.* 932, 172916. doi: 10.1016/j.scitotenv.2024.172916

Ren, Y., Ailierken, A., Zhao, L., Lin, Z., Jiang, J., Li, B., et al. (2022). hUC- MSCs lyophilized powder loaded polysaccharide ulvan driven functional hydrogel for chronic diabetic wound healing. *Carbohydr. Polym.* 288, 119404. doi: 10.1016/j.carbpol.2022.119404

Rizk, M. Z., Aly, H. F., Matloub, A. A., and Fouad, G. I. (2016). The anti-hypercholesterolemic effect of ulvan polysaccharide extracted from the green alga Ulva fasciata on aged hypercholesterolemic rats. *Asian J. Pharm. Clin. Res.* 9, 165–176.

Robic, A., Bertrand, D., Sassi, J. F., Lerat, Y., and Lahaye, M. (2009). Determination of the chemical composition of ulvan, a cell wall polysaccharide from Ulva spp. (Ulvales, Chlorophyta) by FT-IR and chemometrics. *J. Appl. Phycol.* 21, 451–456. doi: 10.1007/s10811-008-9390-9

Roy, A., Roy, P. K., Cho, S. R., and Park, S. Y. (2025). Effects of fucoidan on the inhibition of biofilm formation of Salmonella enterica subsp. enterica serovar Typhimurium on seafoods and its molecular antibiofilm mechanisms. *Microorganisms* 13, 914. doi: 10.3390/microorganisms13040914

Rukmanikrishnan, B., Rajasekharan, S. K., Lee, J., Ramalingam, S., and Lee, J. (2020). K-carrageenan/lignin composite films: biofilm inhibition, antioxidant activity, cytocompatibility, UV and water barrier properties. *Mater. Today Commun.* 24, 101346. doi: 10.1016/j.mtcomm.2020.101346

Shimabukuro, J., Shen, C. L., Hsueh, T. H., Chen, T. W., Tseng, Y., Gannedi, V., et al. (2025). Streamlined synthesis and immunomodulatory effects of ulvan oligosaccharides from marine green algae. *J. Am. Chem. Soc* 147, 32951. doi: 10.1021/jacs.5c09759

Sulastri, E., Lesmana, R., Zubair, M. S., Elamin, K. M., and Wathoni, N. (2021). A comprehensive review on ulvan based hydrogel and its biomedical applications. *Chem. Pharm. Bull.* 69, 432–443. doi: 10.1248/cpb.c20-00763

Sun, Y., Gong, G., Guo, Y., Wang, Z., Song, S., Zhu, B., et al. (2018). Purification, structural features and immunostimulatory activity of novel polysaccharides from Caulerpa lentillifera. *Int. J. Biol. Macromol.* 108, 314–323. doi: 10.1016/j.ijbiomac.2017.12.016

Sun, L., Li, J., Shen, Z., Li, G., Jiang, Y., Chi, Y., et al. (2025). Effect of different extraction methods on the structure and anti-aging skin activity of Ulva pertusa Kjellm polysaccharide. *Carbohydr. Polym. Technol. Appl.* 1, 100969. doi: 10.1016/j.carpta.2025.100969

Tako, M., Tamanaha, M., Tamashiro, Y., and Uechi, S. (2015). Structure of ulvan isolated from the edible green seaweed, Ulva pertusa. *Adv. Biosci. Biotechnol.* 6, 645–655. doi: 10.4236/abb.2015.610068

Tanna, B., and Mishra, A. (2019). Nutraceutical potential of seaweed polysaccharides: structure, bioactivity, safety, and toxicity. *Compr. Rev. Food Sci. Food Saf.* 18, 817–831. doi: 10.1111/1541-4337.12441

Thanh, T. T., Quach, T. M., Nguyen, T. N., Vu Luong, D., Bui, M. L., and Tran, T. T. (2016). Structure and cytotoxic activity of ulvan extracted from green seaweed Ulva lactuca. *Int. J. Biol. Macromolecules.* 93, 695–702. doi: 10.1016/j.ijbiomac.2016.09.040

Tian, H., Yin, X., Zeng, Q., Zhu, L., and Chen, J. (2015). Isolation, structure, and surfactant properties of polysaccharides from Ulva lactuca L. from South China Sea. *Int. J. Biol. Macromol.* 79, 577–582. doi: 10.1016/j.ijbiomac.2015.05.031

Türker, G., Ak, I., Basaran, I., and Keklik, S. (2022). Sulfated polysaccharides from green seaweed Codium tomentosum from Çanakkale Strait (Turkey). *Fresenius. Environ. Bull.* 31, 9148–9157.

Tziveleka, L. A., Pippa, N., Ioannou, E., Demetzos, C., and Roussis, V. (2022). Development of ulvan-containing liposomes as antibacterial drug delivery platforms. *J. Funct. Biomaterials.* 13, 186. doi: 10.3390/jfb13040186

Umamaheswara Rao, M. (1987). Key for the identification of economically important seaweeds. *Bull. Cent. Mainer. Fisheries. Res.* 41, 19–25.

Unuofin, J. O., Otunola, G. A., and Afolayan, A. J. (2018). *In vitro* α-amylase, α-glucosidase, lipase inhibitory and cytotoxic activities of tuber extracts of Kedrostis africana (L.) Cogn. *Heliyon* 4, e00810. doi: 10.1016/j.heliyon.2018.e00810

Usuldin, S. R. A., Wan-Mohtar, W. A. A. Q. I., Ilham, Z., Jamaludin, A. A., Abdullah, N. R., and Rowan, N. (2021). *In vivo* toxicity of bioreactor- grown biomass and exopolysaccharides from Malaysian tiger milk mushroom mycelium for potential future health applications. *Sci. Rep.* 11, 23079. doi: 10.1038/s41598-021-02486-7

Vishwakarma, J., and Sirisha, V. L. (2020). Unraveling the anti-biofilm potential of green algal sulfated polysaccharides against Salmonella enterica and Vibrio harveyi. *Appl. Microbiol. Biotechnol.* 104, 6299–6314. doi: 10.1007/s00253-020-10653-5

Vishwakarma, J., and Vavilala, S. L. (2019). Evaluating the antibacterial and antibiofilm potential of sulphated polysaccharides extracted from green algae Chlamydomonas reinhardtii. *J. Appl. Microbiol.* 127, 1004–1017. doi: 10.1111/jam.14364

Wahlstrom, N., Nylander, F., Malmhäll-Bah, E., Sjövold, K., Edlund, U., Westman, G., et al. (2020). Composition and structure of cell wall ulvans recovered from Ulva spp. along the Swedish west coast. *Carbohydr. Polym.* 233, 115852. doi: 10.1016/j.carbpol.2020.115852

Wang, Y., Chen, L., Wang, Y., Wang, X., Qian, D., Yan, J., et al. (2023). Marine biomaterials in biomedical nano/micro-systems. *J. Nanobiotechnol.* 21, 408. doi: 10.1186/s12951-023-02112-w

Wang, S., and Copeland, L. (2015). Effect of acid hydrolysis on starch structure and functionality: a review. *Crit. Rev. Food Sci. Nutr.* 55, 1081–1097. doi: 10.1080/10408398.2012.684551

Wang, L., Jayawardena, T. U., Yang, H. W., Lee, H. G., Kang, M. C., Sanjeewa, K. K. A., et al. (2020). Isolation, characterization, and antioxidant activity evaluation of a fucoidan from an enzymatic digest of the edible seaweed, Hizikia fusiforme. *Antioxidants* 9, 363. doi: 10.3390/antiox9050363

Xu, J., Liao, W., Liu, Y., Guo, Y., Jiang, S., and Zhao, C. (2023). An overview on the nutritional and bioactive components of green seaweeds Food Production Processing and Nutrition. *Food Prod. Process. Nutr.* 5, 18. doi: 10.1186/s43014-023-00132-5

Yaich, H., Amira, A. B., Abbes, F., Bouaziz, M., Besbes, S., Richel, A., et al. (2017). Effect of extraction procedures on structural, thermal and antioxidant properties of ulvan from Ulva lactuca collected in Monastir coast. *Int. J. Biol. Macromol.* 105, 1430–1439. doi: 10.1016/j.ijbiomac.2017.07.141

Yaich, H., Garna, H., Besbes, S., Barthélemy, J. P., Paquot, M., Blecker, C., et al. (2014). Impact of extraction procedures on the chemical, rheological and textural properties of ulvan from Ulva lactuca of Tunisia coast. *Food Hydrocolloids.* 40, 53–63. doi: 10.1016/j.foodhyd.2014.02.002

Zaharudin, N., Salmeán, A. A., and Dragsted, L. O. (2018). Inhibitory effects of edible seaweeds, polyphenolics and alginates on the activities of porcine pancreatic α-amylase. *Food Chem.* 245, 1196–1203. doi: 10.1016/j.foodchem.2017.11.027

Zhan, H., Yu, G., Zheng, M., Zhu, Y., Ni, H., Oda, T., et al. (2022). Inhibitory effects of a low-molecular-weight sulfated fucose-containing saccharide on α-amylase and α-glucosidase prepared from ascophyllan. *Food. Funct.* 13, 1119–1132. doi: 10.1039/d1fo03331j

Zhang, L., Liao, W., Huang, Y., Wen, Y., Chu, Y., and Zhao, C. (2022). Global seaweed farming and processing in the past 20 years. *Food Prod. Process. Nutr.* 4, 23. doi: 10.1186/s43014-022-00113-0

Zhang, Y., Xu, M., Hu, C., Liu, A., Chen, J., Gu, C., et al. (2019). Sargassum fusiforme fucoidan SP2 extends the lifespan of Drosophila melanogaster by upregulating the Nrf2-mediated antioxidant signaling pathway. *Oxid. Med. Cell. Longevity* 2019, 8918914. doi: 10.1155/2019/8918914